CORE DRILLING OF KO'OLAU VOLCANO REVEALS A RAPID CHANGE IN SHIELD-STAGE GEOCHEMISTRY: IMPLICATIONS FOR COMPOSITIONAL VARIABILITY OF THE HAWAIIAN SOURCE

A THESIS SUBMITTED TO THE GRADUATE DIVISION OF THE UNIVERSITY OF HAWAII IN PARTIAL FULFILLMENT OF THE REQUIREMENTS FOR THE DEGREE OF

MASTER OF SCIENCE

IN

GEOLOGY AND GEOPHYSICS

MAY 2002

By

Eric H. Haskins

Thesis Committee:

Michael O. Garcia, Chairperson
John M. Sinton
Donald Thomas

We certify that we have read this thesis and that, in our opinion, it is satisfactory in scope and quality as a thesis for the degree of Master of Science in Geology and Geophysics.

THESIS COMMITTEE

_____

Chairperson

_____

_____

ACKNOWLEDGEMENTS

I would like to thank the Honolulu Board of Water Supply and geologist Chester Lao for allowing us to core their water observation well in Kalihi Valley. Many thanks to DOSECC drillers Kiki Kama and Vance Hiatt for their tireless work at the KSDP drill site, as well as Bruce Howell, Dennis Nielsen, and Theresa Fall for setting up the drilling operations. Mahalo to David Whilldin, who shared his invaluable experience in order to get the KSDP project rolling. I would also like to thank volunteers Michael G. Davis, Melissa Ito, Toby Vana, and Nathan Adams for their help with core processing. The HSDP and GFZ-Potsdam have been invaluable resources, which provided a template from which I could work on this project and the ability to share so much of it with others. Thank you to the G&G department here at UH for financial support to do glass analyses through a Harold T. Stearns Foundation grant. This project was also financially supported by the NSF, ICDP, University of Hawaii, UC Berkeley, CalTech, MIT, Carnegie Institute of Washington, WHOI, and the Tokyo Institute of Technology. Individuals who have provided invaluable assistance to this project are Michael J. Rhodes and Michael Vollinger for lab use and geochemical analyses, Sarah Bean Sherman for help with analyzing volcanic glass, as well as Eiichi Takahashi, Marc Norman, and Michael J. Rhodes for sharing unpublished data. I would like to extend my deepest gratitide to my thesis committee, composed of Michael O. Garcia, John Sinton, and Don Thomas, for their patience and support throughout this study. Last but not least, family and friends who have provided support in so many ways: Richard and Theresa Vesper, Lisa, Cory, and Abbey Haskins, Steve Sahetapy-Engel, Nathan Becker, and Margaret Milman. This study is in memory of Howard E. Haskins Jr.

TABLE OF CONTENTS

LIST OF TABLES

LIST OF FIGURES

Figure **Page**

INTRODUCTION

The subaerially exposed lavas of Ko'olau volcano on the island of O'ahu are geochemically distinct among Hawaiian shield volcanoes in their major and trace elements, as well as isotopic compositions. One of their distinctive features is high SiO_2, which cannot be produced by melting of mantle peridotite (Lassiter & Hauri, 1998). Instead, the distinct geochemistry of Ko'olau is thought to be the result of a source component containing recycled oceanic crust (Frey et al., 1994; Hauri et al., 1996). The continuity of this distinctive geochemistry within Ko'olau volcano has been questioned in several recent studies. Work on flows exposed deep within a new highway tunnel (Jackson et al., 1999) and from the submarine flanks of Ko'olau volcano (Tanaka et al., 2002; Shinozaki et al., 2002) have unexpectedly revealed compositions resembling Kilauea and Mauna Loa, respectively.

These findings suggest that the geochemically distinct lavas of Ko'olau form only a thin veneer over more typical Hawaiian tholeiites. If this hypothesis is correct, then obtaining lava samples beneath the exposed surface of the volcano could reveal a geochemical transition within the main growth stage of a Hawaiian volcano. We anticipated that scientific drilling on the leeward side of the Ko'olau range would not only produce less altered samples better suited for geochemical analyses and dating, but also an excellent stratigraphic section for paleomagnetic studies. Although the shield-stage geochemical stratigraphy of most Hawaiian shields is incompletely known, such a transition within Ko'olau would be in sharp contrast with the relatively uniform major element compositions of Kilauea and Mauna Loa shield-stage lavas over time (Quane et al., 2000; Rhodes, 1996).

The Ko'olau Scientific Drilling Project (KSDP) was initiated in the spring of 2000 to evaluate whether the interior of the Ko'olau shield is geochemically distinct from surface lavas, and if so, to determine the nature of this transition and the geochemical evolution of the upper part of the shield. This project utilized a groundwater observation well drilled in 1999 from 46.8 m above sea level (masl) to 304 m below sea level (mbsl) for the Honolulu Board of Water Supply (HBWS) in Kalihi Valley. Sampling rock fragments from this depth interval and core from 304 – 632 mbsl allowed us to examine and analyze lavas from deeper stratigraphic levels than are exposed subaerially.

Upon completion of drilling, detailed core logging and petrographic examination of both rock cuttings and core revealed unexpected and variable rock types as well as fresh glass in KSDP lavas. Major element analyses show that KSDP rocks and glasses are geochemically distinct from typical Ko'olau lavas; they bear a closer resemblance to lavas from Mauna Loa volcano. KSDP incompatible trace element compositions are intermediate between Mauna Loa and Ko'olau, showing more subtle differences in source magma composition. Dating of KSDP samples indicates that shield-stage Ko'olau lavas are older than previously thought. The transition from typical Ko'olau to Mauna Loa-like lavas is characterized as relatively abrupt (~60 m thick). The depth of the KSDP geochemical transition is slightly shallower than expected based on its location in the H3 tunnel section, near the Ko'olau caldera rim. It is difficult to assess whether this discrepancy is the result of the differential subsidence that all Hawaiian volcanoes experience (Moore, 1987), or simply the result of minor flank slope variations. The high SiO_2 and incompatible trace element abundances as well as Os isotopic evidence (Hauri et al., 1996) point to increasing incorporation of recycled oceanic crust in the Ko'olau

source during the late shield-stage growth of this volcano. Experimental studies melting ancient oceanic crust and peridotite have sought to create the source melts of Hawaiian volcanoes (e.g., Takahashi & Nakajima, 2002). The crystallization paths of these potential parental magma compositions were modeled using MELTS. These paths were compared to those of representative melt inclusions in olivine from Ko'olau and Mauna Loa picrites, as well as evaluated against KSDP, Ko'olau, and Mauna Loa major element glass compositions. None of the experimental melts produce tholeiitic compositions that consistently match any Hawaiian volcano. In contrast, the average composition of melt inclusions in olivine from Ko'olau and Mauna Loa picrites can be modeled successfully as a parental composition.

GEOLOGIC SETTING

The extinct Ko'olau volcano makes up the eastern part of the island of O'ahu in the Hawaiian archipelago. Its lavas, dated by K-Ar methods at ~1.8 – 2.6 Ma (Doell & Dalrymple, 1973), overlie those of the adjacent Waianae volcano [K-Ar ages from ~2.9 – 3.9 Ma (Doell & Dalrymple, 1973; Presley et al., 1997, Guillou et al., 2000)]. The subaerially exposed remains of these deeply eroded volcanoes preserve their basic elongate shield form (Fig. 1). The Ko'olau shield is constructed entirely of tholeiitic basalt lava flows that currently reach a maximum elevation of 932 masl (Macdonald et al., 1983). Some of the major geologic features of the subaerial Ko'olau shield are its rift zones (with associated dike complexes), and its caldera complex (Fig. 1). A 64 km-long NW-trending rift and a shorter, ESE-trending one that extends beyond Makapu'u Head

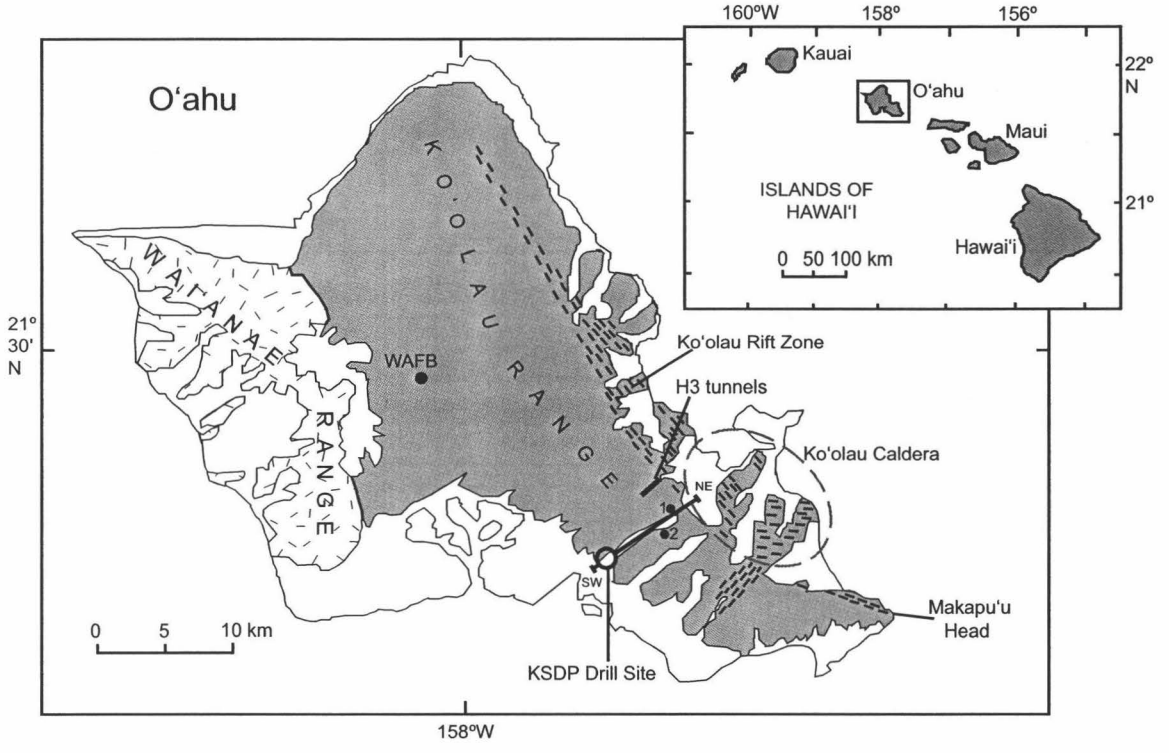

Fig. 1. Geologic map of the island of O'ahu, containing the eroded remnants of Ko'olau (gray) and Waianae (hatched) volcanoes (modified from Jackson et al., 1999) Major features of Ko'olau such as the rift zones and caldera are shown, as well as previous study sites (Makapu'u Head, H3 tunnels, and the Wheeler Air Force Base - WAFB). The KSDP drill site is located in lower Kalihi valley. The location for the cross section (Fig. 2) is shown by the line labeled SW-NE. Locations labeled 1 and 2 are rejuvenated vent locations Kalihi and Kamanaiki flows, respectively. The inset map shows the island of O'ahu among the Hawaiian islands.

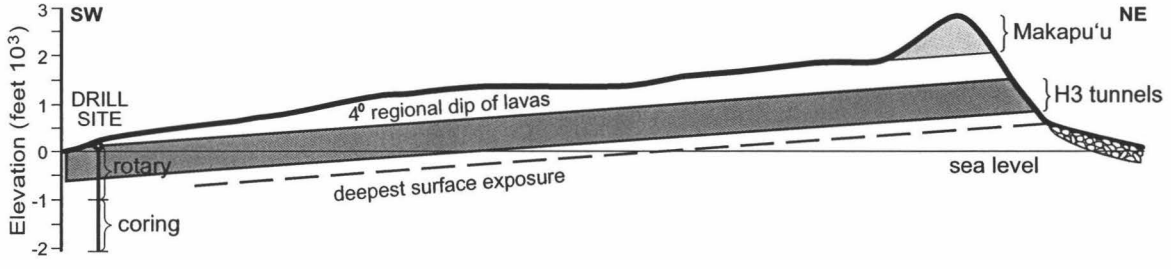

Fig. 2. Cross section of Kalihi valley showing the relative stratigraphic positions of previous studies projected to the drill site using the 4° regional dip observed in the H3 tunnels (Jackson et al., 1999). The deepest surface exposure is also projected.

both emanate from the now deeply eroded caldera (Stearns, 1939; Wentworth & Jones, 1940; Walker, 1986). A catastrophic event, the Nu'uanu landslide, is thought to have carried away most of the eastern portion ($2.9 - 3.8 \times 10^3$ km^3) of Ko'olau volcano and littered the seafloor with giant blocks up to 40 km long for distances up to 150 km (Moore et al., 1989).

No evidence has been found on Ko'olau of post-shield lavas, which usually mark the final period of pre-erosional growth of typical Hawaiian volcanoes (Macdonald, 1963). Other Hawaiian volcanoes (e.g., West Molokai'i and Lana'i) also have little or no evidence of this stage of Hawaiian volcanism (Macdonald et al., 1983). No model has been proposed to explain the absence of this stage, but a possible link may be the fact that these three volcanoes all produced large and catastrophic debris avalanches during or shortly after their main growth stage (Moore et al., 1989, Moore et al., 1994).

After ~1 Ma of erosion and at least 1 km of subsidence of the Ko'olau shield (Clague & Dalrymple, 1987; Moore, 1987), rejuvenated-stage eruptions began. Rejuvenated activity produced numerous monogenetic eruptions of strongly silica undersaturated magma from 874 ±6 ka to 33 ±3 ka (Gramlich et al., 1971). This material is commonly referred to as the Honolulu Volcanic Series (Winchell, 1947).

Kalihi Valley Drill Site Regional Geology

The KSDP drill site (Fig. 1) is located on the western margin of lower Kalihi Valley at an elevation of ~47 m. Although outcrops of tholeiitic flows are only ~50 m away from the site, these flows do not lie immediately beneath the alluvial surface. Kalihi Valley was incised into the Ko'olau shield and later partially filled by nepheline

melilitite lavas from two rejuvenated-stage eruptions (Stearns & Vaksvik, 1935; Wentworth, 1951). Rejuvenated-stage flows are also observed in other Honolulu valleys including Nu'uanu, Pauoa, and Mānoa (Stearns & Vaksvik, 1935).

The older Kalihi flow erupted from a vent just southwest of Pu'u Kahuauli (Fig. 1, location 1), and can be traced down the valley to an elevation of ~67 m where alluvium conceals its lower reaches. K-Ar dates of the Kalihi flow are 470 ±12 ka (Gramlich et al., 1971) and 580 ±25 ka (Lanphere & Dalrymple, 1980). Later rejuvenated flows erupted from one or more vents on the ridge between Kamanaiki and Kalihi valleys (Fig. 1, location 2), and are referred to as the Kamanaiki flows. These flows, which traveled down both sides of the ridge and into lower Kalihi (Stearns & Vaksvik, 1935; Wentworth, 1951), contain slightly more melilite and less pyroxene and nepheline than the Kalihi flow (Winchell, 1947). The Kamanaiki eruption has not been dated, but both Stearns & Vaksvik (1935) and Winchell (1947) determined that it occurred during the same time period as the Black Point and Punchbowl eruptions, which were dated by two different studies: 480 ±80 and 530 ±40 ka, respectively (Lanphere & Dalrymple, 1980), and 302 ±5 and 304 ±5 ka, respectively (Gramlich et al., 1971). The Kamanaiki lava extends ~6 km seaward from its vent complex, forming a wide apron under the Kalihi Kai coastal plain (Stearns, 1939; Winchell, 1947). The locations of contacts between the Kalihi and Kamanaiki flows within the valley are unknown.

The relative position of the KSDP drill site below the volcano's paleo-shield surface can be estimated using the slopes of Ko'olau's leeward ridges, adjusted for erosion. Wentworth and Winchell (1947) used these ridges to make an estimate of the

maximum extent of shield growth. Subtraction of the KSDP drill site elevation from this maximum indicates that drilling began 100 – 200 m below the pre-erosional surface.

The stratigraphic height of the drill site with respect to previous Ko'olau studies was estimated by constructing a cross section of the southwest flank of the volcano (Fig. 2). At the H3 tunnels, near the crest of the Ko'olau range, a regional lava flow dip of 4° was measured (Jackson et al., 1999). The opposite end of the cross section was placed at the KSDP drill site, ~7.6 km away. Lava flow contacts and internal flow dips were measured near the drill site and up the valley for ~2 km at ridge outcrops. Individual flow dips are variable (0.5-8°) due to irregular underlying surface flow topography, so an attempt was made to measure average dips and thereby minimize surface irregularity. Internal flow boundaries ('a'ā shear zones showing parallel vesicle lineations and pāhoehoe shear zones marked by abrupt vertical changes in vesicularity) were measured in areas with significant flow surface variability.

The average dip of flows in lower Kalihi Valley is ~4° (Table 1), in agreement with the regional dip estimate from the H3 tunnels (Jackson et al., 1999). However, Kalihi lava flow dips decrease with depth from 6° to 3° over the ~70 m composite section. A previous study of Ko'olau lavas on the leeward flanks of the volcano (Multhaup, 1990) also noted a decrease in dip with depth, both by geochemical correlation of rock cuttings from eight closely located drill holes in Waipahu (Fig. 1, location 3) and dip measurements of flows exposed by excavation for house lots from the southwest portion of Wa'ahila Ridge (Fig. 1, location 4). At the former location, dips plunge up to x° back toward the center of the volcano at depth, and at the latter they

Table 1. Dip measurements of lava flows from the western flank of lower Kalihi Valley. Measurements taken to the nearest half degree and arranged in order of relative stratigraphic height for a ~70 m composite section.

Depth in Section	Avg. Dip	No. of Meas.	Surface measured
Upper	6.0°	3	thin pāhoehoe flow contacts
	6.0°	2	shear zone separating vesicularity bands within a pāhoehoe flow
	5.0°	2	top contact of an 'a'ā flow
	4.8°	3	strained vesicles within a massive 'a'ā flow
	4.5°	2	strained vesicles within a massive 'a'ā flow
	4.5°	4	strained vesicles within a massive 'a'ā flow
	3.5°	2	pāhoehoe over 'a'ā flow contact
	3.5°	2	shear zone separating vesicularity bands within a pāhoehoe flow
	5.0°	2	shear zone separating vesicularity bands within a pāhoehoe flow
	3.5°	2	shear zone separating vesicularity bands within a pāhoehoe flow
	3.5°	2	shear zone separating vesicularity bands within a pāhoehoe flow
	3.0°	3	pāhoehoe intraflow contacts
Lower	3.0°	4	a series of three thin pāhoehoe flows
Average	4.3°		

Table 2. Summary of flow type, lithology, and flow thickness (m) for KSDP rock cores.

Flow Type	No. of Flows	Picritic Basalts	Olivine Basalts	Basalts	Total Thickness	Mean Thickness	Vol%
'a'ā	15	3	2	10	46.5	3.1	14.2
pāhoehoe	67	7	17	43	211.9	3.2	64.7
transitional	19	1	3	15	58.5	3.1	17.9
massive	2	2	0	0	10.7	5.3	3.3
total	103	13	22	67	327.6	3.2	100.0

Picritic Basalt = >12% olivine, Olivine Basalt = 5-12% olivine, Basalt = <5% olivine

decrease systematically down section from 5° to 1.8° over only 30.5 m. Jackson et al. (1999) reported only the average dip measured at the H3 tunnels, with no mention of dip changes with depth.

Based on our cross section of Ko'olau through Kalihi Valley (Fig. 2), it was anticipated that the rotary-drilling phase of the KSDP would sample lavas of similar stratigraphic intervals as the Makapu'u and upper H3 tunnel sections. Core drilling was expected to extend at least 300 m beyond the stratigraphic equivalent of the deepest Ko'olau surface exposure. The flows cored would therefore sample deeper portions of the volcano than any previous study including the H3 tunnels, and allow us to evaluate the suggestion of Jackson et al. (1999) – that the geochemically distinct lavas of Ko'olau volcano may be a relatively thin surface feature covering lava with more typical Hawaiian compositions.

METHODS

Rotary and Core Drilling

Rotary drilling of the HBWS groundwater observation well began in late summer of 1999 and was completed on October 6 of the same year. Water Resources International, Inc. used a Spencer-Harris Model 3500 drilling rig to reach a depth of 303.7 mbsl (350.5 m total depth; Fig. 3). The well diameter is 38.1 cm to a depth of ~4 masl, and 20 cm from this depth to the bottom of the hole. Permanent casing with an inner diameter of 20.3 cm and 0.8 cm wall thickness was installed in the wide, upper portion of the well and grouted in place. Drillers sampled rock cuttings at 2-3 m intervals, although no cuttings were returned from the 90 - 173 mbsl depth interval.

Fig. 3. DOSECC's GLAD 800 coring system (not to scale, rig ~10 m tall) and the KSDP borehole plan. (scale =1:4950).

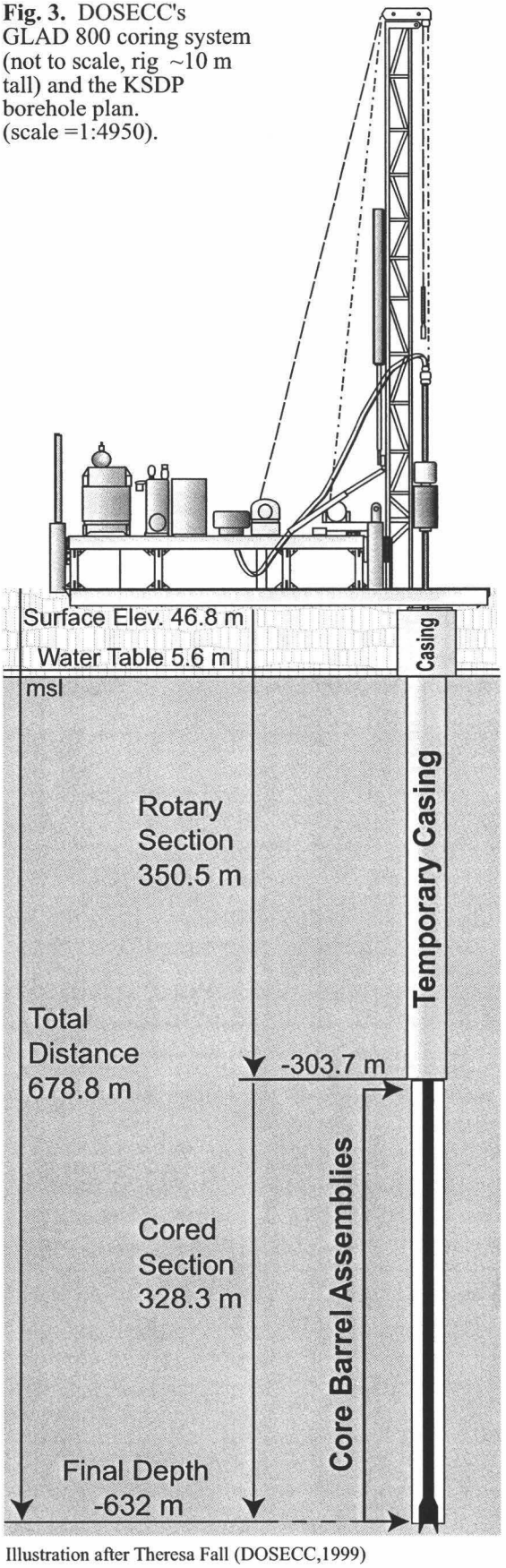

Illustration after Theresa Fall (DOSECC,1999)

Samples were sieved at ~10 m intervals, separating fragments larger than 2 mm to be washed. A binocular microscope was used to examine and select unaltered samples for thin section petrography and XRF major element analyses. A total of 26 intervals were selected for thin sections, spaced roughly evenly.

The KSDP rock coring took place only on weekdays, 8 am – 5 pm between April 14 and May 24, 2000. The restricted drilling time was necessary because the drill site is located adjacent to a residential area. Core drilling services were provided by DOSECC (Drilling, Observation, and Sampling of the Earth's Continental Crust) using their newly built GLAD800 rig. Drill rig specifications are given at the DOSECC website at http://www.dosecc.org/GLAD800/glad800.html. A plan view of the drill site layout is shown in Fig. 4. In order to preserve the integrity of the water observation well, temporary casing was installed from the surface to the bottom of the rotary-drilled section before core drilling began. The coring utilized a 9.3 cm outer diameter diamond drill bit of to cut the rock and produce core of 6.1 cm diameter. As the rock was cut and the bit advanced, core sample was fed into a ~3 m barrel. When this barrel was full or blocked, it was pulled to the surface by a wire line while the core bit and rods remained in the hole. Core was extracted from the barrel and placed in a pair of plastic trays, each two meters in length and marked for vertical orientation. The rock was rinsed with water to remove drilling mud and small particles of core created during drilling or extraction from the barrel. Preliminary examinations and descriptions of the core were conducted to aid later and more detailed logging efforts (see Appendix). The core was pieced together, marked for logging orientation, boxed, and then transported to the logging area where it was split, dried, digitally photographed, marked again on its new split surface, described

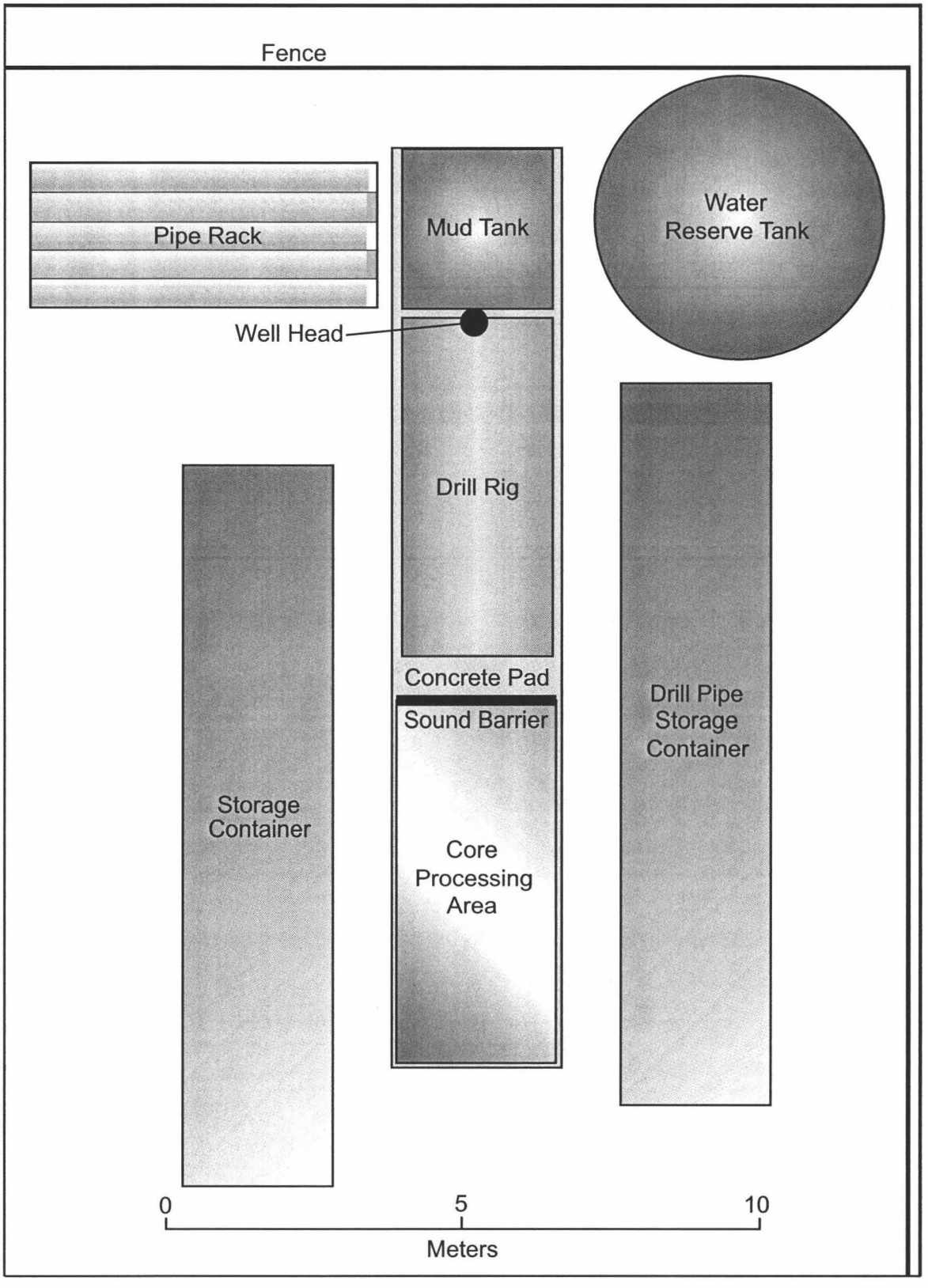

Fig. 4. Plan view of the KSDP drill site. All drilling materials including the drill rig were shipped to Honolulu and assembled on site. The concrete pad was constructed for the rotary drill rig and reused for the GLAD 800 coring interval.

in hand specimen, and sampled for thin section and geochemical analysis. Core handling and logging was conducted according to procedures developed during the Hawaii Scientific Drilling Project (HSDP). These procedures are summarized below, with a more detailed decription located in the Appendix.

Petrologic Logging

The KSDP penetrated ~679 m, reaching a final depth of 632 mbsl. The main focus of petrologic logging was the rock core. For each lithologic unit, the flow and intraflow contacts were noted (if present), as well as groundmass size, vesicularity, extent of alteration, fracturing, and other outstanding features. Internal and external flow features such as autoliths, flow banding, ropy pāhoehoe surface textures, and volcanic glass were commonly preserved and confirm that KSDP core samples generally experienced less weathering than surface Ko'olau lavas.

During petrologic logging, each unit was point counted with a transparent sheet containing a 100-point overlay grid to determine the visible mineral (olivine and/or plagioclase) and vesicle abundances. The same rock was point counted by another petrographer to verify the first count. Point count results that varied ≤2 vol% were averaged. Larger differences necessitated point recounts, until loggers reached agreement within 2 vol%. A modified IUGS (Le Maitre et al., 1989) rock classification scheme was used, wherein a description of vesicularity was included in the rock name along with mineral abundance information from point counting (e.g. moderately vesicular, highly plagioclase olivine-phyric basalt) based on the aforementioned descriptive information. Lithologic units were assigned unit types ('a'ā, pāhoehoe,

transitional, or massive) based on their characteristics (e.g., ʻaʻā flows generally have elongate vesicles and a massive core between layers of clinker, pāhoehoe flows have spherical vesicles and often contain multiple lobes, transitional flows have characteristics of both ʻaʻā and pāhoehoe, and massive flows have no vesicles).

The presence or absence of soil, baked material, or glassy surfaces was used to define flow and intraflow contacts. These contacts were annotated on box photographs, as well as locations where point counts were taken, unit numbers, and other notable features (see Appendix for an example of logging forms). Detailed logging descriptions, box photographs, daily reports of drilling activities, and additional information about the KSDP can be found at http://icdp.gfz-potsdam.de/html/Koolau/news.html.

Geochemical Analyses

Whole-rock major and trace element abundances from the KSDP (Tables 3 & 4) were determined by X-ray fluorescence (XRF) at the University of Massachusetts (UMass). This laboratory conducted most of the previous analyses of Koʻolau lavas, so analyses for rocks from areas of the volcano can be compared without concern for interlaboratory bias. Major elements were determined in duplicate with a Siemens MRS-400 multi-channel, simultaneous X-ray spectrometer with an internal standard to maintain analytical precision. Within the rotary-drilled section, the least altered fragments of a uniform rock type were selected from each depth interval. A minimum number (1-8 fragments) was used to obtain the 300 mg of powder required for one major element analysis. These chips were treated in an ultrasonic bath until clean and powdered in an alumina mortar before being sent to UMass for analysis.

Table 3. XRF whole-rock major element analyses for KSDP lavas. Shaded rows indicate altered samples (K_2O/P_2O_5 <1.2 or >2.2 and/or LOI >0.8) not shown in geochemical variation diagrams. *total iron as Fe_2O_3, - = no data All values are in weight%

Unit	Depth (m)	SiO_2	TiO_2	Al_2O_3	Fe_2O_3*	MnO	MgO	CaO	Na_2O	K_2O	P_2O_5	Total	LOI
Rotary-Drilled Section													
-	~50	52.31	1.77	13.68	11.46	0.16	8.88	8.81	2.56	0.12	0.22	99.99	1.27
-	0.4	52.48	1.67	13.79	10.98	0.16	8.63	8.90	2.54	0.23	0.22	99.59	-
-	-62.9	52.11	2.24	14.56	11.49	0.15	6.25	9.41	2.71	0.38	0.32	99.62	-
-	-88.8	52.36	2.07	14.57	11.17	0.15	6.43	10.00	2.74	0.40	0.29	100.17	-
-	-181.8	49.06	2.33	14.62	12.33	0.16	7.82	10.61	2.36	0.11	0.30	99.70	-
-	-209.2	52.67	1.80	13.20	11.05	0.16	8.88	8.81	2.45	0.43	0.25	99.69	-
-	-212.3	50.30	2.25	14.60	11.95	0.17	7.65	10.59	2.36	0.14	0.29	100.30	0.11
-	-215.3	53.60	1.89	14.03	10.65	0.15	7.10	9.25	2.61	0.44	0.26	99.98	0.19
-	-218.4	50.05	2.32	14.56	12.38	0.18	7.48	10.72	2.39	0.23	0.31	100.61	1.13
-	-221.4	50.41	2.30	14.40	12.23	0.18	7.29	10.64	2.32	0.11	0.32	100.18	0.80
-	-224.5	50.37	2.28	14.72	12.10	0.18	7.20	10.50	2.25	0.12	0.29	100.00	1.56
-	-227.5	51.30	2.19	14.01	11.71	0.17	7.31	10.45	2.39	0.23	0.26	100.02	0.28
-	-230.6	48.99	2.70	15.10	12.22	0.17	7.00	10.78	2.40	0.24	0.35	99.94	0.79
-	-233.6	50.97	2.25	14.47	11.95	0.17	7.36	10.61	2.31	0.15	0.25	100.49	0.48
-	-236.7	50.87	2.33	14.44	12.03	0.17	6.92	10.57	2.42	0.16	0.26	100.17	0.67
-	-244.3	49.94	2.47	14.21	12.31	0.17	7.18	10.68	2.49	0.20	0.27	99.92	-
-	-268.7	49.07	2.25	12.83	12.55	0.18	10.21	9.96	2.13	0.19	0.25	99.61	-
-	-303.7	50.75	2.31	13.33	12.27	0.18	7.95	10.23	2.23	0.34	0.26	99.85	-
Cored Section													
1	-303.8	49.34	1.59	11.32	11.72	0.17	15.42	8.20	1.94	0.27	0.18	100.15	0.16
2	-308.4	48.14	1.36	9.87	12.30	0.17	18.62	7.23	1.65	0.15	0.16	99.64	-0.02
3	-308.9	49.27	1.54	10.95	11.83	0.17	15.95	7.95	1.83	0.26	0.18	99.92	0.16
4	-312.3	51.78	1.85	13.28	11.12	0.16	9.52	9.29	2.33	0.23	0.21	99.77	0.16
5	-314.4	50.36	1.56	11.37	11.50	0.16	14.55	7.90	1.91	0.22	0.19	99.71	0.26
6	-316.6	50.14	1.54	11.22	11.53	0.16	15.07	7.87	1.89	0.29	0.18	99.90	0.09
7	-325.0	50.35	1.98	12.54	11.91	0.17	10.65	9.45	1.93	0.38	0.20	99.58	0.50
8	-329.0	50.40	1.97	12.08	11.86	0.17	11.53	9.25	2.11	0.38	0.23	99.98	0.13
9	-332.4	52.60	1.70	13.22	11.34	0.17	9.19	9.18	2.38	0.26	0.17	100.21	0.03
10	-334.2	52.10	1.71	13.22	11.36	0.17	9.07	9.20	2.35	0.21	0.16	99.53	0.14
12	-336.0	52.12	1.70	13.12	11.42	0.17	9.41	9.13	2.35	0.30	0.16	99.88	1.83
13	-338.0	50.79	2.34	13.48	12.22	0.18	7.82	10.47	2.22	0.50	0.27	100.28	0.41
14	-341.9	50.65	2.33	13.43	12.15	0.17	7.92	10.46	2.30	0.51	0.28	100.20	0.22
15	-343.8	50.97	2.02	12.86	12.28	0.17	9.49	9.62	2.20	0.40	0.22	100.23	-0.02
16	-345.5	50.35	2.50	13.46	12.44	0.17	7.46	10.69	2.02	0.45	0.28	99.83	0.17
17	-350.4	50.97	2.30	13.75	12.05	0.17	7.51	10.49	2.23	0.42	0.25	100.13	0.26
18	-355.6	50.30	2.36	13.81	12.20	0.17	7.31	10.70	2.23	0.43	0.27	99.78	0.27
19	-357.8	50.88	2.44	13.86	12.07	0.17	7.05	10.76	2.30	0.52	0.29	100.33	0.17
20	-359.2	49.13	1.94	11.47	12.28	0.17	13.66	8.95	1.85	0.44	0.22	100.12	0.13
21	-362.5	51.30	2.30	14.36	11.82	0.17	6.89	10.30	2.17	0.18	0.20	99.69	1.03
22	-363.9	52.25	2.09	14.11	11.15	0.17	7.15	10.45	2.37	0.38	0.24	100.36	0.16
23	-367.3	52.07	2.15	13.95	11.66	0.18	7.20	10.13	2.28	0.36	0.21	100.17	0.47
24	-370.6	52.20	2.13	13.74	11.64	0.17	7.18	10.05	2.42	0.37	0.23	100.12	0.01
25	-372.5	51.93	2.13	13.79	11.70	0.17	7.26	10.10	2.38	0.32	0.22	100.00	0.01
26	-376.1	51.62	2.24	13.67	11.76	0.17	7.53	10.37	2.29	0.43	0.25	100.32	1.76
27	-379.5	51.76	2.22	14.09	11.34	0.17	6.88	10.55	2.35	0.32	0.24	99.91	0.24
28	-379.8	51.96	2.25	14.05	11.33	0.17	6.58	10.48	2.29	0.45	0.25	99.79	0.16
29	-381.3	49.21	1.91	12.03	12.42	0.18	12.81	9.06	2.00	0.31	0.20	100.13	0.41
30	-383.0	50.59	1.97	12.32	12.05	0.18	11.39	9.28	1.98	0.28	0.23	100.27	0.36
31	-387.6	46.89	1.34	8.49	13.19	0.18	21.74	6.47	1.57	0.20	0.14	100.20	0.09
32	-388.2	49.30	1.91	11.97	12.37	0.18	12.73	8.98	2.06	0.22	0.19	99.92	0.25
33	-390.0	50.47	2.23	13.41	12.10	0.18	8.77	10.26	2.05	0.27	0.20	99.92	0.63
34	-391.4	50.48	2.14	12.96	12.13	0.18	9.64	10.07	2.22	0.28	0.20	100.31	0.11
35	-392.0	51.25	2.24	13.32	11.96	0.18	8.48	10.25	2.13	0.25	0.24	100.29	0.34

Table 3 (cont.).

Unit	Depth (m)	SiO_2	TiO_2	Al_2O_3	Fe_2O_3*	MnO	MgO	CaO	Na_2O	K_2O	P_2O_5	Total	LOI
36	-394.4	49.67	2.10	12.64	12.58	0.19	10.55	9.72	2.10	0.25	0.18	99.97	0.38
37	-395.8	50.85	2.25	13.52	12.00	0.18	8.07	10.67	2.22	0.38	0.25	100.37	-0.07
38	-398.6	51.21	2.32	13.50	12.11	0.18	7.60	10.59	2.23	0.31	0.22	100.27	0.35
39	-403.8	50.66	2.42	13.45	12.49	0.18	7.62	10.72	2.17	0.38	0.23	100.31	0.16
40	-407.6	50.46	2.34	13.24	12.43	0.18	8.05	10.58	2.18	0.36	0.22	100.04	0.24
41	-408.8	50.63	2.39	13.41	12.34	0.18	7.38	10.72	2.34	0.32	0.23	99.94	0.11
44	-411.2	50.76	2.38	13.54	12.24	0.18	7.35	10.75	2.31	0.40	0.24	100.15	0.03
45	-412.3	50.25	2.06	12.19	12.17	0.18	11.04	9.35	2.14	0.40	0.22	100.00	-0.02
46	-413.6	51.36	2.26	13.61	11.68	0.17	7.58	10.44	2.43	0.38	0.23	100.14	0.36
47	-418.8	51.24	2.22	13.59	11.58	0.18	7.46	10.41	2.42	0.41	0.24	99.74	0.18
48	-422.7	51.58	2.29	13.82	11.53	0.17	6.87	10.59	2.71	0.44	0.25	100.25	0.12
49	-426.1	51.25	2.18	13.62	11.79	0.18	7.41	10.65	2.47	0.34	0.21	100.09	-0.01
50	-429.7	51.02	2.10	12.68	11.82	0.17	9.79	9.51	2.45	0.38	0.22	100.14	0.09
51	-433.4	51.45	2.25	13.77	11.64	0.17	7.56	10.40	2.31	0.36	0.20	100.13	0.28
52	-438.9	49.74	1.97	12.33	11.85	0.18	11.36	9.25	2.31	0.33	0.21	99.53	0.08
53	-440.4	50.09	1.95	12.25	11.90	0.18	12.02	8.94	2.31	0.37	0.20	100.20	0.38
54	-443.7	51.25	2.40	13.78	11.80	0.18	6.95	10.72	2.53	0.40	0.25	100.26	0.22
55	-445.7	49.65	2.52	14.28	12.16	0.18	6.92	11.01	2.49	0.22	0.17	99.59	0.72
56	-448.8	50.94	2.33	13.92	11.69	0.18	7.04	10.93	2.60	0.32	0.25	100.20	0.09
57	-453.2	51.05	2.35	13.77	11.89	0.18	7.37	10.60	2.44	0.36	0.23	100.23	0.17
59	-456.1	51.36	2.39	13.73	11.74	0.17	7.12	10.55	2.51	0.49	0.26	100.32	0.16
60	-464.5	50.88	2.54	14.03	12.01	0.18	6.45	10.29	2.68	0.27	0.25	99.58	0.15
61	-469.3	51.27	2.29	13.79	11.71	0.17	7.34	10.23	2.57	0.42	0.25	100.04	-0.01
62	-476.4	50.93	2.23	12.98	11.97	0.18	8.68	10.23	2.33	0.38	0.23	100.12	0.07
63	-482.1	51.57	2.31	13.66	11.66	0.17	6.90	10.34	2.57	0.47	0.25	99.90	-0.09
64	-493.4	51.66	1.67	12.61	11.51	0.17	10.76	9.28	2.30	0.25	0.16	100.38	-0.10
65	-495.9	51.19	1.95	12.49	11.81	0.17	10.02	9.47	2.36	0.34	0.21	100.01	0.01
66	-506.9	51.23	2.09	13.03	11.48	0.17	8.60	9.92	2.46	0.42	0.22	99.63	-0.02
67	-511.0	51.89	1.87	13.15	11.35	0.17	8.78	9.42	2.62	0.31	0.17	99.71	0.09
68	-514.2	50.80	1.98	12.84	11.69	0.17	10.09	9.39	2.48	0.26	0.18	99.89	0.07
69	-521.8	52.29	2.03	13.91	11.13	0.18	7.02	10.00	2.74	0.29	0.17	99.75	0.19
70	-526.0	52.35	2.00	13.90	11.53	0.17	8.02	9.73	2.24	0.25	0.13	100.32	0.76
71	-526.5	51.97	2.06	13.71	11.56	0.18	8.17	10.02	2.17	0.31	0.15	100.28	0.34
72	-533.7	52.18	2.17	13.89	11.39	0.17	7.20	10.33	2.32	0.27	0.23	100.15	0.18
73	-535.2	51.24	2.23	13.95	11.50	0.17	7.06	10.54	2.59	0.27	0.22	99.77	0.19
74	-537.9	52.15	2.14	13.95	11.44	0.17	7.23	10.33	2.25	0.31	0.18	100.14	0.35
75	-544.9	51.72	2.18	13.70	11.60	0.18	7.21	10.32	2.30	0.36	0.23	99.79	-0.07
76	-550.3	48.66	2.32	13.25	12.44	0.19	9.62	10.68	2.34	0.18	0.12	99.78	0.43
81	-556.4	49.66	2.25	14.47	11.98	0.17	7.64	10.39	2.46	0.38	0.09	99.49	1.38
82	-558.7	50.37	2.29	13.98	11.95	0.18	7.11	10.73	2.65	0.19	0.23	99.67	0.19
83	-562.0	49.39	2.30	14.36	12.30	0.18	7.72	10.99	2.22	0.19	0.21	99.85	1.15
85	-564.8	50.06	2.17	14.07	12.18	0.16	8.50	9.72	2.26	0.24	0.19	99.55	2.89
88	-569.4	48.89	1.80	12.60	12.46	0.26	13.02	8.19	2.03	0.19	0.17	99.61	3.65
91	-573.7	49.22	2.57	13.81	12.28	0.19	8.34	11.20	2.09	0.19	0.27	100.14	1.55
92	-581.7	46.63	1.58	9.22	12.62	0.19	21.11	6.68	1.59	0.14	0.17	99.95	2.63
93	-586.4	50.62	2.33	14.18	11.68	0.18	7.12	10.93	2.6	0.15	0.24	100.03	0.33
94	-590.4	51.21	2.17	13.71	11.06	0.17	8.46	10.43	2.42	0.14	0.21	99.99	0.80
95	-593.7	50.65	2.21	13.75	11.50	0.17	8.21	10.55	2.45	0.20	0.19	99.87	0.60
96	-596.0	51.34	2.03	13.79	10.81	0.17	8.26	10.64	2.34	0.12	0.21	99.70	0.74
97	-597.7	47.24	2.12	11.21	13.02	0.20	15.63	8.96	1.37	0.13	0.22	100.09	2.95
98	-600.3	48.75	2.39	13.80	12.22	0.18	8.75	11.12	2.15	0.16	0.20	99.71	1.44
100	-606.3	50.20	2.29	13.86	12.00	0.18	7.72	11.44	2.05	0.21	0.24	100.18	0.96
101	-622.3	50.78	2.01	13.69	11.17	0.17	8.21	10.95	2.43	0.18	0.20	99.79	0.52
102	-625.5	50.80	2.19	13.32	11.73	0.18	7.98	10.63	2.38	0.22	0.21	99.63	0.54

Table 4. XRF whole-rock trace element analyses for KSDP lavas. All values are in ppm.

Unit	Depth (m)	V	Cr	Ni	Zn	Rb	Sr	Y	Zr	Nb	Ba	Ce
Rotary-Drilled Section												
-	~50	204	551	239	111	0.8	317	21.4	109	6.6	111	19
Cored Section												
1	-303.8	193	746	596	104	3.0	267	17.7	101	7.0	64	19
2	-308.4	175	797	769	109	1.7	235	15.3	86	6.0	66	19
3	-308.9	183	717	594	105	3.4	256	17.2	96	6.6	61	20
4	-312.3	205	608	234	104	2.5	324	20.2	121	7.5	72	25
5	-314.4	175	801	576	105	2.4	272	17.4	102	6.2	72	17
6	-316.6	179	794	588	104	3.6	272	17.3	101	6.1	63	19
7	-325.0	229	718	315	110	4.4	302	20.9	126	8.0	70	21
8	-329.0	225	638	361	104	4.7	308	21.6	127	8.1	69	26
9	-332.4	193	478	163	98	3.5	268	20.6	104	6.5	56	18
10	-334.2	200	517	166	103	2.0	266	20.0	104	6.7	64	19
12	-336.0	208	504	164	103	3.3	267	19.9	106	6.8	63	19
13	-338.0	257	341	105	108	6.8	374	23.7	154	10.5	94	28
14	-341.9	257	331	102	106	7.1	377	24.0	154	10.5	94	33
15	-343.8	236	522	210	108	5.4	307	21.7	127	9.3	85	25
16	-345.5	268	337	103	106	6.6	392	24.3	161	11.5	103	30
17	-350.4	254	348	104	112	5.7	351	23.7	143	10.4	90	24
18	-355.6	254	284	102	107	5.6	380	24.2	153	10.8	86	32
19	-357.8	259	277	82	105	6.2	382	24.7	157	11.0	96	29
20	-359.2	225	735	471	107	5.4	307	20.1	128	9.3	82	26
21	-362.5	246	260	75	108	1.6	355	23.3	148	10.1	103	27
22	-363.9	231	289	78	98	5.0	352	22.4	133	8.9	86	27
23	-367.3	237	333	80	108	4.4	334	23.7	138	9.3	79	29
24	-370.6	241	291	79	106	4.8	337	23.6	139	9.1	74	26
25	-372.5	238	279	80	106	3.9	335	23.2	137	9.1	84	25
26	-376.1	238	289	93	101	5.7	353	24.1	145	9.5	86	29
27	-379.5	238	298	88	103	4.2	355	24.1	144	9.6	84	28
28	-379.8	237	288	84	106	6.0	351	23.5	147	9.9	87	27
29	-381.3	222	756	388	110	3.9	305	20.6	126	8.4	71	24
30	-383.0	217	734	331	108	4.5	311	22.2	129	8.7	87	25
31	-387.6	159	938	973	110	1.8	219	14.3	88	5.8	60	18
32	-388.2	213	776	392	111	2.3	305	19.9	124	8.2	75	26
33	-390.0	239	525	177	110	3.7	318	22.7	138	9.5	84	27
34	-391.4	234	512	194	99	3.5	322	22.6	135	9.2	85	25
35	-392.0	240	495	157	109	3.0	323	24.4	140	9.4	87	24
36	-394.4	235	602	243	113	2.9	308	21.7	132	8.9	82	25
37	-395.8	256	404	126	109	4.5	336	24.0	142	9.7	82	28
38	-398.6	246	377	116	107	4.7	336	23.8	146	10.0	86	25
39	-403.8	268	363	103	113	4.4	337	24.7	151	10.4	90	29
40	-407.6	241	421	125	111	4.3	329	24.2	146	10.2	78	25
41	-408.8	241	340	91	108	3.7	337	25.8	149	10.3	82	22
44	-411.2	250	323	82	105	4.4	337	24.9	150	10.4	86	27
45	-412.3	227	710	282	107	4.4	309	21.9	133	9.0	74	25
46	-413.6	249	338	112	112	5.0	348	23.1	144	9.9	101	28
47	-418.8	249	311	109	100	5.2	351	23.2	143	9.7	85	30
48	-422.7	248	267	78	104	5.5	355	23.6	148	10.4	87	28
49	-426.1	233	316	97	97	4.3	334	22.7	138	9.2	71	28
50	-429.7	218	519	188	106	4.8	358	21.0	141	10.0	104	26
51	-433.4	249	366	100	102	4.8	343	23.5	144	9.1	77	27
52	-438.9	222	492	342	108	4.4	318	21.0	127	9.3	86	25
53	-440.4	197	473	364	104	5.0	308	20.3	125	9.0	91	23
54	-443.7	244	263	78	103	5.4	369	24.7	153	11.5	112	29
55	-445.7	263	253	82	115	2.6	375	24.4	159	12.2	106	30
56	-448.8	249	268	81	108	4.6	373	23.8	149	11.3	116	28

Table 4 (cont.).

Unit	Depth (m)	V	Cr	Ni	Zn	Rb	Sr	Y	Zr	Nb	Ba	Ce
57	-453.2	234	290	92	105	5.0	366	23.6	150	11.2	114	30
59	-456.1	235	292	86	104	6.3	361	24.5	151	11.2	102	28
60	-464.5	248	228	84	109	2.6	366	26.3	160	12.6	119	28
61	-469.3	237	323	113	97	5.9	354	23.7	144	11.0	101	30
62	-476.4	231	415	148	100	5.8	331	22.2	129	10.2	104	28
63	-482.1	238	290	91	99	6.7	347	24.2	143	11.2	105	29
64	-493.4	197	585	253	94	3.6	267	18.9	98	6.6	64	20
65	-495.9	216	576	232	98	4.7	296	21.0	118	7.9	75	24
66	-506.9	223	446	160	97	5.4	320	22.0	131	9.2	79	26
67	-511.0	205	427	133	98	4.0	293	20.6	116	7.7	65	20
68	-514.2	214	532	240	104	3.2	322	21.4	126	8.2	80	26
69	-521.8	227	295	87	102	4.5	304	23.6	126	8.2	75	22
70	-526.0	213	355	118	107	2.7	307	21.0	122	8.0	283	22
71	-526.5	223	345	123	101	4.3	312	22.6	128	8.5	82	23
72	-533.7	234	254	80	99	3.0	322	23.8	136	9.1	77	22
73	-535.2	244	300	82	106	3.5	332	24.3	143	9.4	92	26
74	-537.9	234	297	78	103	4.3	327	22.7	136	8.8	99	24
75	-544.9	223	309	72	97	5.6	320	23.8	138	8.9	81	25
76	-550.3	270	542	215	112	1.9	308	22.0	139	9.1	84	26
81	-556.4	256	342	130	117	8.9	318	24.0	141	9.6	226	24
82	-558.7	242	266	84	106	2.1	334	26.1	143	9.2	86	30
83	-562.0	267	336	133	116	2.4	335	26.3	144	9.6	65	29
85	-564.8	234	477	210	135	2.8	281	23.4	132	10.7	114	28
88	-569.4	176	615	436	109	3.0	222	19.0	104	8.2	108	23
91	-573.7	278	395	149	117	2.4	378	25.2	166	13.9	159	39
92	-581.7	174	995	912	114	2.1	188	16.3	94	7.7	287	17
93	-586.4	264	317	101	107	1.9	332	24.7	143	9.7	119	26
94	-590.4	244	472	184	114	1.3	332	23.4	127	8.3	65	23
95	-593.7	247	439	171	103	1.6	330	23.1	130	8.7	56	25
96	-596.0	237	469	165	111	1.2	330	21.8	119	8.1	68	21
97	-597.7	222	831	582	113	1.9	236	20.3	121	9.4	102	22
98	-600.3	269	492	158	115	1.7	304	24.2	136	10.4	85	26
100	-606.3	246	301	137	102	3.4	321	24.7	140	9.7	61	28
101	-622.3	241	432	158	92	2.9	308	21.5	121	8.6	50	23
102	-625.5	229	416	154	93	3.9	310	23.0	129	9.2	77	26

Core samples from the freshest portions of the least altered flows (88 of the 104 identified lithologic units) were selected for geochemical analysis. For comparison, a basalt sample was taken from the entrance arch in the bypass tunnel adjacent to the drill site. Samples were ground in an agate shatterbox. Coarse sample fragments were flushed with water for a minimum of 5 days until the conductivity of the water stabilized. Samples were then sonified 3-4 times in deionized water or until a background conductivity of 1-2 microsiemens was reached. Dried samples were ignited overnight and powdered in an agate mortar before being weighed out for analysis.

Each core sample was prepared in duplicate and fused with a lithium tetraborate flux. Major element precision and accuracy for SiO_2, TiO_2, Al_2O_3, Fe_2O_3, MgO, CaO, and K_2O is typically better than 0.5% for Hawaiian tholeiitic basalts, except MnO, Na_2O, and P_2O_5, which are typically within 0.5-1% (1σ error; Rhodes, 1996). Loss on ignition (LOI) was determined by heating approximately 5 g of sample in a Pt:Au (95:5) crucible at 1020°C for at least 10 hours. Only 500 mg of rock was used for LOI analysis of the rotary section cuttings due to the limited amount of material available.

Whole-rock trace element abundances for KSDP study sites were determined in duplicate using a Philips PW2400 sequential spectrometer. Powder pellets were pressed for each sample using the procedures of Norrish and Hutton (1969) and Chappell (1991). Trace element (V, Cr, Ni, Zn, Rb, Sr, Y, Zr, Nb, Ba, and Ce) precision and accuracy at 1σ is typically within 0.5-2% (Rhodes, 1996).

Volcanic glass major element abundances from KSDP flow and intraflow contacts (Table 5) were determined by electron microprobe analysis at the University of Hawaii at Mānoa using a five spectrometer, Cameca SX-50 electron microprobe. Natural glass and

Table 5. Microprobe analyses of major elements in KSDP glasses.

Sample Depth (m)	Rock Unit	# of Analyses	SiO_2	TiO_2	Al_2O_3	FeO*	MnO	MgO	CaO	Na_2O	K_2O	P_2O_5	Total
-324.3	7	4	52.82	2.32	14.42	10.21	0.12	6.40	10.65	2.22	0.44	0.22	99.61
-326.6	8	28	52.47	2.23	14.18	9.99	0.17	6.91	10.57	2.41	0.41	0.21	99.33
-353.3	17	18	52.33	2.61	13.77	11.18	0.22	6.28	10.53	2.62	0.34	0.27	99.87
-366.2	22	25	52.80	2.20	14.27	10.31	0.17	6.52	10.31	2.53	0.40	0.20	99.50
-373.9	26	9	53.28	2.64	13.71	11.29	0.17	5.85	10.09	2.33	0.28	0.24	99.65
-377.1	27	4	52.96	2.49	13.78	10.95	0.16	6.25	10.59	2.40	0.38	0.24	99.95
-381.1	29	5	52.31	2.51	13.88	10.91	0.16	6.30	10.36	2.09	0.47	0.25	99.26
-389.9	33	7	51.36	2.34	14.25	10.59	0.15	7.11	10.88	2.13	0.40	0.21	99.41
-402.7	39	6	50.97	2.81	13.66	11.80	0.16	6.06	10.74	2.37	0.44	0.25	99.27
-409.0	42	5	51.20	2.50	14.12	10.81	0.21	7.01	11.14	2.57	0.40	0.20	100.16
-419.3	47	6	52.13	2.59	13.88	11.19	0.17	6.41	10.64	1.65	0.49	0.24	99.41
-432.4	50	4	52.39	2.39	14.26	10.09	0.11	6.46	10.62	2.37	0.50	0.23	99.42
-445.5	55	4	51.66	2.72	13.74	11.15	0.14	6.25	10.62	2.27	0.50	0.25	99.30
-446.3	56	4	51.52	2.75	13.83	11.51	0.12	6.07	10.38	2.29	0.54	0.29	99.29
-449.8	57	4	51.96	2.91	13.40	11.16	0.24	6.22	10.32	2.62	0.72	0.25	99.80
-459.9	60	4	52.21	3.21	13.05	12.25	0.20	5.27	9.75	2.57	0.60	0.28	99.38
-480.6	63	5	51.82	2.90	13.47	11.81	0.18	5.74	10.01	2.22	0.55	0.27	98.97
-512.6	67	5	52.99	2.28	13.98	10.50	0.16	6.17	10.13	2.18	0.40	0.24	99.03
-539.4	74	7	52.16	2.32	13.98	10.67	0.16	6.33	10.51	2.34	0.44	0.25	99.16
-588.3	94	9	52.46	2.37	14.27	10.44	0.16	6.88	10.83	1.44	0.38	0.20	99.42
-615.6	101	6	51.02	2.36	14.27	10.39	0.17	7.08	10.98	2.37	0.36	0.23	99.21

*all iron as FeO Shaded rows indicate samples with significant Na_2O loss.

mineral standards (VG2, A99, OR-1, and Apatite 1) were used for calibration. A PAP-ZAF correction was applied to all analyses and minor corrections (<2%) were made based on 5-10 repeated analyses of Smithsonian glass standards A99 and VG2 (Jarosewich et al., 1979) run both before and after analysis of unknowns. A 10 μm diameter, 10 nA beam current and 15 kV accelerating voltage was used for each 150 s analysis. Peak counting times were 60 s for Fe, Ti, Al, and P; 50 s for Si and Mg; and 40 s for Ca, Na, Mn, and K. Backgrounds were measured for half the peak counting intervals, except for Ti and K (20 and 30 s background intervals, respectively). To minimize volatilization, Na data was acquired during the first of two spectrometer alignments needed for each analysis. Reported data are an average of 4-28 analyses from each depth, depending on glass abundance in each sample. Analytical errors based on counting statistics are within 0.1 wt% for all oxides except SiO_2, CaO, and FeO, which are within 0.25 wt%.

Geochronology

Ko'olau surface lavas have been subjected to tropical weathering (Frey et al., 1994). Due to this alteration, K-Ar dates for Ko'olau lavas from even a single site are commonly inconsistent (e.g., different cores from the same flow give ages up to 1 Ma apart; Doell & Dalrymple, 1973). The most reliable K-Ar age determinations for this volcano range from 1.8 – 2.6 Ma (Doell & Dalrymple, 1973; Lanphere & Dalrymple, 1980). All published paleomagnetic analyses of Ko'olau lavas show reversed polarity, which indicates eruption in the early Matuyama (0.73 – 2.58 Ma; Cande & Kent, 1995). Before our study, there were no Ar-Ar ages for Ko'olau lavas. The relatively unaltered

nature of KSDP flows prompted us to undertake Ar-Ar dating of core rocks to obtain more accurate dates for subaerially erupted Ko'olau flows.

Strict criteria were applied to the selection of samples for Ar-Ar dating. KSDP Units 14, 19, and 66 were selected based on their relatively unaltered appearance (AI <3), relatively high K abundance (>0.4 wt % K_2O), and unaltered geochemistry (K_2O/P_2O_5 >1.5 and <0.3 wt% LOI; see the Postmagmatic Alteration Effects section below for discussion of these criteria). These samples have a holocrystalline groundmass and <10% vesicularity. Units 14 and 19 are the least altered units from the top of the core section; Unit 66 is one of the least altered flows with relatively high K_2O at significant depth in the section. Samples were sent to the Oregon State University (OSU) geochronology laboratory for analysis, and prepared according to procedures described in Sinton et al., (1996). The new Ar-Ar age determinations are shown in Table 6.

RESULTS

Rotary-Drilled Section Stratigraphy

The first rock chips were sampled at ~36 masl, beneath alluvial soils (Fig. 5). Thin section examinations of these rocks sampled throughout the rotary-drilled section revealed up to 4 rock types. Generally, there is a dominance of one or two rock types within each depth interval, which probably represent the thickest flow(s) intersected. The estimated unit boundaries and relative phenocryst abundances were estimated for the most abundant rock types (Fig. 5). These considerations and the large depth interval with no sample recovery resulted in a low-resolution stratigraphy for this portion of the KSDP.

Rock cuttings from the shallowest portion of the well are almost entirely

Table 6. Results from ^{40}Ar-^{39}Ar radiometric dating.

Depth (mbsl)	Unit	Incremental Heating (°C)	Plateau Age ± 2σ (Ma)	% ^{39}Ar	MSWD	Normal Isochron Age ± 2σ (Ma)	$^{40}Ar/^{36}Ar_i$† ± 2σ	MSWD	Inverse Isochron Age ± 2σ (Ma)	$^{40}Ar/^{36}Ar_i$ ± 2σ	MSWD
341.9	14	600* 700* 800* 950* 1100 1250 1400	2.89 ± 0.12	82.0	0.73	2.89 ± 0.55	295.4 ± 12.3	1.16	2.90 ± 0.53	295.3 ± 11.8	1.09
357.8	19	600* 750* 850* 950* 1100 1250 1400	2.83 ± 0.16	88.0	0.06	2.73 ± 0.74	297.8 ± 17.0	0.05	2.72 ± 0.74	297.8 ± 16.9	0.05
506.9	66	600* 800* 900* 1000* 1100* 1250* 1400	2.90 ± 0.22	97.7	0.89	2.98 ± 0.55	294.4 ± 6.3	1.12	3.00 ± 0.53	294.4 ± 6.2	1.07

*Heating steps used in the plateau and isochron age calculations.

†Initial $^{40}Ar/^{36}Ar$ based on the inverse of the y-intercept of the regression.

MSWD (Mean Square of Weighted Deviates) describes how well the data are fit by the isochron (a perfect fit MSWD = 1)

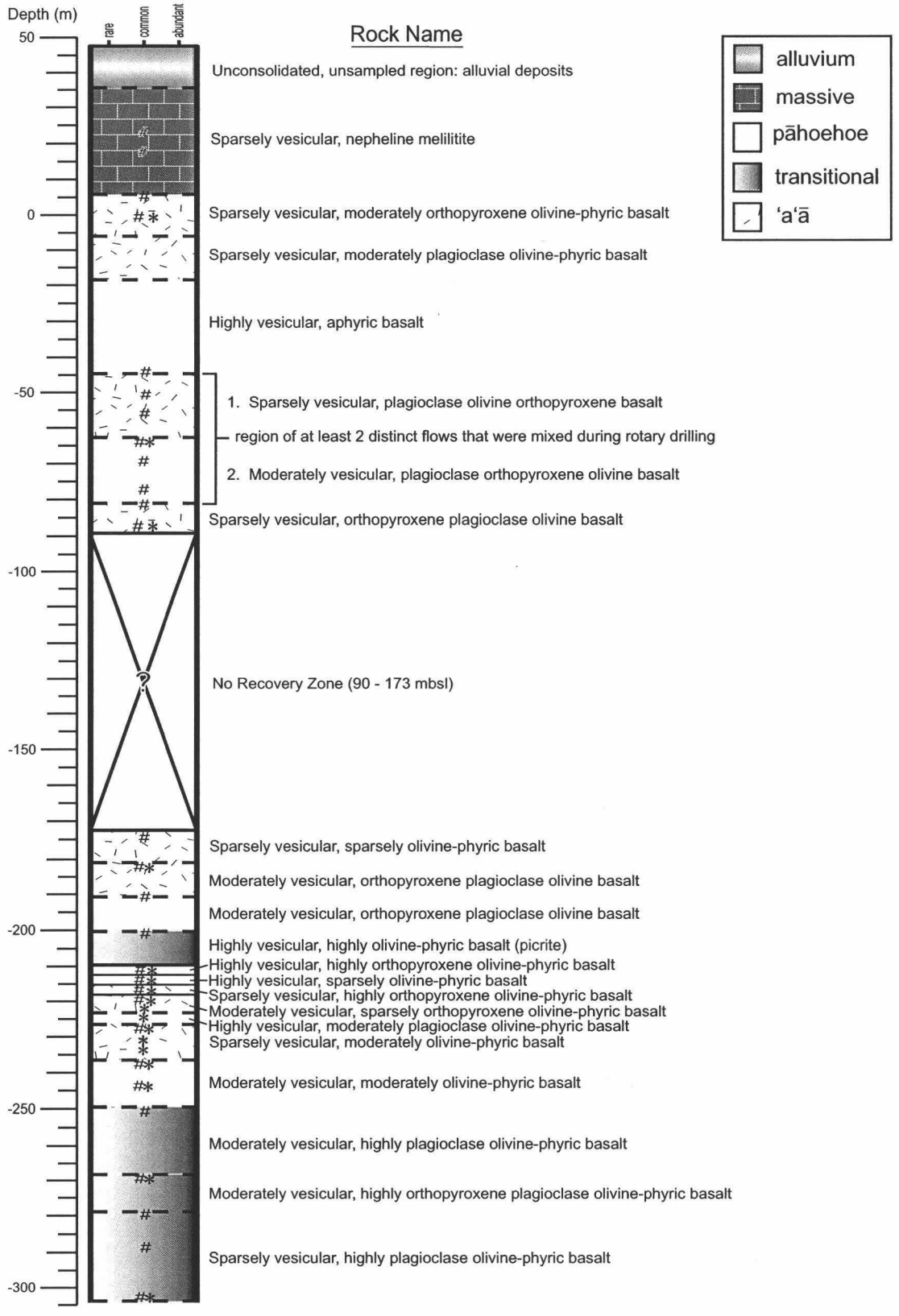

Fig. 5. Graphic log for the KSDP rotary-drilled interval. Dashed lines indicate discernable flow boundaries. Rock names determined from thin section examination are listed next to each identified unit. Symbols # and * denote thin section and XRF sample locations, respectively.

nepheline melilitites to a depth of ~5 masl (Table 7). There is no change in primary mineralogy with depth, although there is an increase in the abundance of altered rock fragments. A small piece of abraded coral and a shell (each ~5 mm) were found among the rock cuttings at 18 m, and another coral fragment (~8 mm) was recovered 25 m lower. These findings are consistent with driller observations of coral from the same depths, but the scarcity of coralline material sampled indicates that no paleo-reefs were sampled below the drill site. Due to the mixed nature of the rock returned by rotary drilling, the lack of information concerning flow boundary locations, and the petrographic similarity of the two Kalihi nepheline melilitite flows, we were unable to determine whether only one or both of the rejuvenated flows were sampled. Kalihi and Kamanakiki flows can be differentiated geochemically (Clague & Frey, 1982), but there were not enough unaltered rock fragments sampled from this depth interval for XRF analysis.

Beneath the rejuvenated flows lie Ko'olau shield-stage lavas (Fig. 5). Rotary drilling obscures flow contacts, making it impossible to determine the number of flows intersected within the depth interval from ~6 masl to 302 mbsl. Distinct flows are difficult to identify from 2-20 mm-wide cuttings, particularly within the large sampling interval (minimum ~3 m). Only 18 shield-stage units were identified by petrographic and geochemical methods. Previous measurements (Wentworth and Winchell, 1947) of many hundreds of subaerially exposed Ko'olau lavas indicate an average flow thickness of ~3 m. Recent studies (Frey et al., 1994; Jackson et al., 1999) of near-vent flow sequences found average flow thicknesses of 2.1 and 1.6 m, respectively. Flows sampled by KSDP coring ~7.6 km from their probable caldera source vent have an average thickness of 3.2

Table 7. Lithology of rock cuttings from the rotary-drilled section of the KSDP.

Depth (m)	%Abundance	Flow type	ol	opx	plag	cpx	other
23.9	100	massive	C	N	N	N	nepheline, melilite
17.8	100	massive	C	N	N	N	nepheline, melilite
5.7	50	massive	C	N	N	N	nepheline, melilite, calcite
	50	ʻaʻā	C	C	N	mph	N
-0.4	90*	ʻaʻā	C	C	N	mph	N
	10	massive	C	N	N	N	nepheline, melilite, calcite
-44.6	80	pāhoehoe	N	N	C	mph	N
	10	ʻaʻā	N	N	C	N	N
	5	?	?	?	?	?	?
	5	glass	mph	mph	mph	N	N
-50.7	45	ʻaʻā	N	C	C	N	N
	45	pāhoehoe	C	N	C	mph	N
	10	?	C	N	N	N	N
-56.8	60	pāhoehoe	C	N	mph	mph	N
	40	ʻaʻā	C	C	N	N	N
-62.9	90*	pāhoehoe	C	C	N	N	N
	10	ʻaʻā	C	C	C	N	N
-69.0	70	ʻaʻā	R	C	R	N	N
	25	pāhoehoe	C	N	R	mph	N
	5	massive	C	N	N	N	nepheline, melilite
-76.6	75	ʻaʻā	N	R	C	N	N
	20	pāhoehoe	C	N	C	N	N
	5	massive	C	N	N	N	nepheline, melilite
-81.2	95	ʻaʻā	C	N	C	N	N
	5	pāhoehoe	N	N	mph	mph	N
-88.8	100*	transitional	N	R	C	N	N
----------No Recovery Zone (NRZ)----------							
-172.7	100	ʻaʻā	R	N	N	N	N
-181.8	100*	ʻaʻā	R	R	R	N	N
-190.9	55	pāhoehoe	C	N	C	mph	N
	45	ʻaʻā	C	R	C	N	N
-200.1	100	transitional	C	N	mph	mph	N
-209.2	100*	pāhoehoe	C	C	N	N	N
-212.3	100*	pāhoehoe	R	N	mph	mph	N
-215.3	100*	ʻaʻā	C	C	mph	mph	N
-218.4	100*	ʻaʻā	C	R	N	N	N
-221.4	*	-	-	-	-	-	-
-224.5	*	-	-	-	-	-	-
-227.5	80*	ʻaʻā	C	N	mph	N	N
	20	pāhoehoe	C	N	mph	N	N
-230.6	*	-	-	-	-	-	-
-233.6	*	-	-	-	-	-	-
-236.7	90*	pāhoehoe	C	N	mph	mph	N
	10	ʻaʻā	C	N	N	N	N
-244.3	100*	pāhoehoe	C	N	mph	mph	N
-250.4	100	transitional	C	N	C	mph	N
-268.7	100*	transitional	C	R	C	N	N
-279.3	100	transitional	C	R	C	N	N
-288.5	100	transitional	C	N	C	mph	N
-303.7	95*	pāhoehoe	C	N	C	N	N
	5	?	C	R	C	N	N

Phenocrysts: C = Common, R = Rare, N = None, mph = microphenocrysts. *XRF samp.
ol = olivine, opx = orthopyroxene, plag = plagioclase, cpx = clinopyroxene. - = no data.

m (Table 2). Assuming this KSDP average flow thickness value, the 308 m rotary-drilled section represents ~96 flows. Not only is the KSDP rotary section's sampling interval insufficient to discern thin lava flows, rotary drilling makes consecutive units with identical lithology virtually indistinguishable. The absence of 24% of the section (no cuttings returned from ~90-170 mbsl) further underscores the problematic nature of rotary drilling for scientific study.

Petrography – Rotary Section

Rock mineralogy, flow type, and degree of alteration were estimated for the rotary section cuttings from thin section examinations (Table 7). The nepheline melilitites contain abundant olivine and common melilite phenocrysts up to 3 mm long, with nepheline and opaque microphenocrysts. Secondary clay minerals and calcite are rare but increase to 10 vol% with depth. The petrographic similarity of the Kalihi and Kamanaiki lavas (Winchell, 1947) prevents us from distinguishing these flows, even after thin section examination.

Ko'olau basalts underlie the nepheline melilitites. In the rotary-drilled section, they range in lithology from aphyric to porphyritic lavas. Flow type estimates are based mainly on groundmass texture, vesicle shape and abundance, and textural relationships. Pāhoehoe lavas generally have a microcrystalline groundmass, abundant undeformed vesicles, and occasionally exhibit diktytaxitic texture. 'A'ā usually has a cryptocrystalline groundmass and elongate vesicles. The dense interiors of 'a'ā flows generally have <10 vol% vesicles. Transitional flows have intermediate characteristics of

both flow types, but lack diktytaxitic texture. These flow type features also are observed in KSDP core thin sections.

Olivine is the dominant phenocryst phase in KSDP rotary section lavas, although some rock fragments contain only phenocrysts of orthopyroxene and/or plagioclase (Table 7). Many olivine phenocrysts are skeletal, indicating rapid cooling. Even in the freshest sections olivine is slightly altered, with thin iddingsite rims ~0.2 mm. Olivine in some lavas is dark in color from minute iron oxide inclusions. Such features are indicative of baking (Haggerty and Baker, 1967).

The common presence of orthopyroxene phenocrysts in the KSDP rotary section rocks is typical of Ko'olau basalts, and thought to be the result of their high SiO_2 compared to other Hawaiian volcanoes (Wentworth and Winchell, 1947). In the WAFB section, orthopyroxene is present in 27 of the 35 Ko'olau basalts (77%) sampled (Takahashi & Takeguchi, in review). Orthopyroxene phenocrysts are unaltered, large (0.5 - 8 mm), and present in 17 of 28 Ko'olau chip samples examined (Table 7), particularly in the upper 2/3 of the section. Below 215 mbsl, orthopyroxene is rare to absent. Plagioclase is common throughout the rotary-drilled portion of the hole, occurring as unaltered phenocrysts, microphenocrysts, and in the groundmass. Phenocrysts of plagioclase are more abundant (but still secondary to olivine) toward the bottom of the section, particularly from 250 to 300 mbsl. Clinopyroxene and opaque phases are present only as microphenocrysts and in the groundmass. Of particular interest are four consecutive sections from 209, 212, 215, and 218 mbsl, which have all been analyzed by XRF (Table 3). Each of these sections is petrographically uniform and distinct from the other three with respect to crystallinity, vesicularity, mineral occurrence,

and mineral abundance. These findings suggest that each sampling depth provided cuttings from a different flow, each ~3 m thick. Overall, all lavas from the rotary-drilled section appear petrographically similar to subaerially exposed Ko'olau rocks (e.g., Wentworth & Winchell, 1947; Frey et al., 1994).

Cored Section Stratigraphy

Core recovery for KSDP was high (~95%), filling 112 core boxes with 103 subaerially erupted lava flows and one sedimentary unit (Table 2, Fig. 6). Pāhoehoe is the dominant flow type both in total thickness and number of flows, including two intervals in the middle of the section with 12 and 13 consecutive pāhoehoe units. Flow thickness is generally independent of flow type, as many pāhoehoe units were inflated after emplacement or are compound flows composed of multiple lobes. There are 13 picritic flows (>12 wt% MgO and >15% olivine), of which 38.5% are dense 'a'ā or massive units. The latter represents a disproportionate excess compared to the 16.5% overall abundance of 'a'ā flows. Olivine basalts and basalts (containing 5 – 15 vol% and <5 vol% olivine, respectively) are more common, with basalts forming the majority of lavas sampled regardless of flow type. A thin (1 m) non-volcanic unit composed of fluvial sandstone was found deep in the section (566 mbsl). Most flows above this unit appear relatively unaltered or weakly altered. Below this unit, all of the flows appear moderately to strongly altered (Tables 3 & 8).

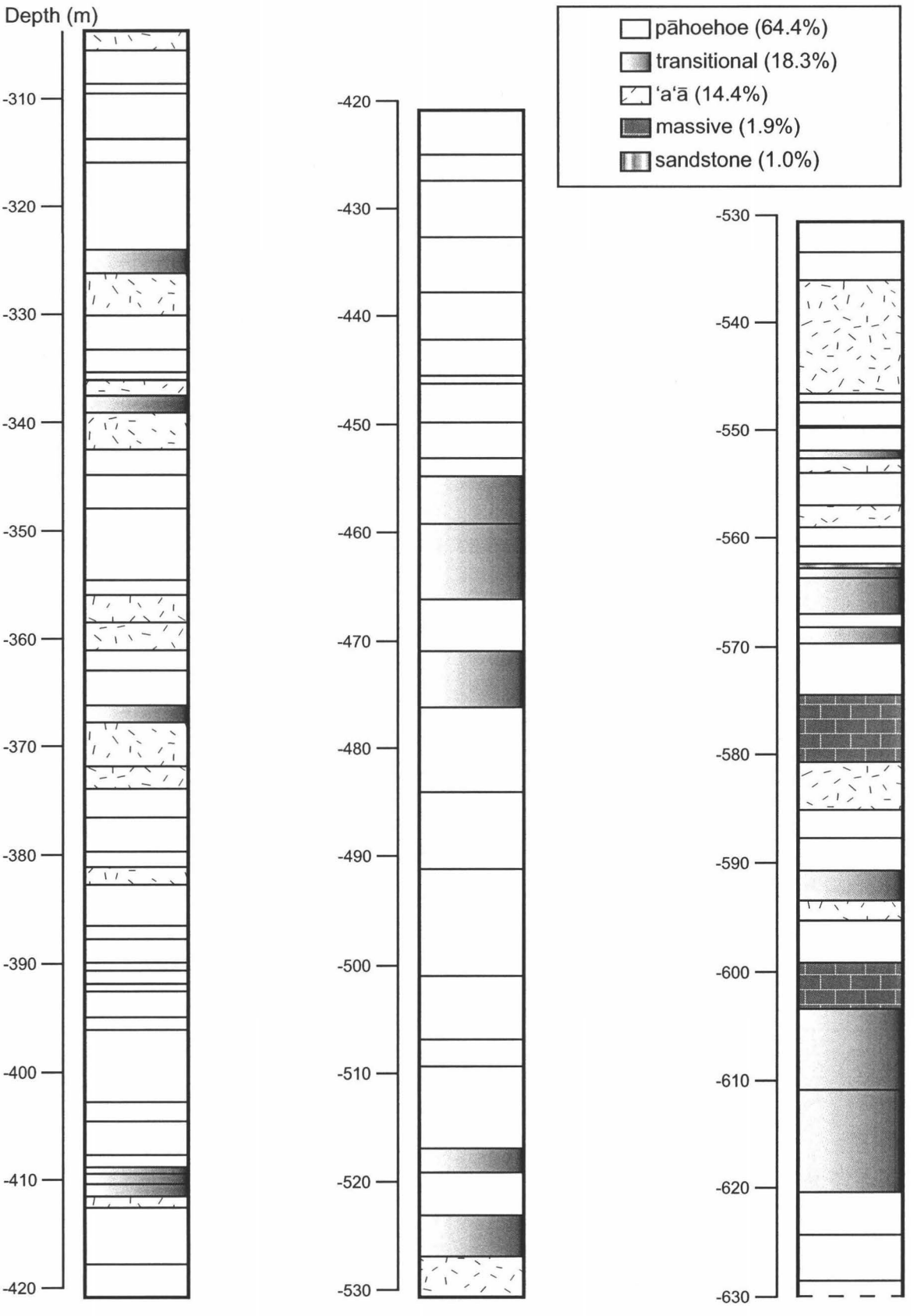

Fig. 6. The KSDP cored interval. All 104 units are shown, with flow type occurrence noted.

Table 8. Vesicle-free modal mineralogy (volume %, based on 500-point counts) and crystallization sequences for KSDP lavas from the cored interval.

Unit	Depth	Gmass	ol		opx		plag		cpx		opq	A.I.	Crystallization
	(m)	(%, c/m)	ph	mph	ph	mph	ph	mph	ph	mph	mph	(1-5)	Sequence
1	-303.8	65.0,c	20.2	-	3.2	-	9.6	-	2.0	-	-	2	ol,pl,opx,cpx
2	-308.3	56.2,m	26.6	-	4.6	-	7.0	3.2	1.6	0.8	-	2.5	ol,pl,opx,cpx
3	-308.9	49.4,m	32.8	-	4.6	-	5.4	4.2	2.2	1.4	-	3	ol,pl,opx,cpx
4	-312.3	85.2,c	7.8	-	-	-	-	5.4	-	1.2	0.4	2.5	ol,pl,opx,cpx
5	-314.5	81.6,c	17.8	-	-	-	-	-	0.6	-	-	3	ol,cpx,pl
6	-316.8	79.4,c	20.0	-	-	-	-	0.4	-	-	0.2	2.5	ol,pl
7	-325.3	87.4,c	12.4	-	-	-	-	-	-	-	0.2	2.5	ol,pl±cpx
8	-329.0	86.4,c	10.8	-	-	-	0.2	2.2	-	0.4	-	1.5	ol,pl,cpx
9	-332.4	90.2,c	5.6	-	2.4	0.8	0.2	0.6	-	-	0.2	2	ol,opx,pl,cpx
10	-334.5	93.6,c	3.4	-	3.0	-	-	-	-	-	-	3	ol,opx,pl±cpx
12	-336.2	92.4,c	2.0	-	4.6	-	-	1.0	-	-	-	2.5	ol,opx,pl,cpx
13	-338.0	94.6,c	3.0	-	-	-	0.2	2.2	-	-	-	2.5	ol,pl,cpx
14	-342.0	90.8,c	5.2	-	-	-	0.2	2.8	0.2	0.8	-	2	ol,pl,cpx
15	-343.9	81.6,m	10.4	-	-	-	0.2	4.6	-	3	0.2	2.5	ol,pl,cpx
16	-345.5	91.0,c	2.0	-	-	-	-	3.8	1.0	1.8	0.4	2.5	ol,pl±cpx
17	-350.4	97.2,c	1.2	-	-	-	0.8	0.2	-	0.6	-	1.5	ol,pl,cpx
18	-355.6	84.2,c	9.6	0.4	-	-	-	3.0	-	2.2	0.6	3	ol,pl±cpx
19	-358.0	94.4,c	2.2	-	-	-	0.8	1.2	0.6	0.8	-	2	ol,pl±cpx
20	-359.2	82.0,c	16.2	-	-	-	0.4	0.6	0.4	0.4	-	2	ol,pl,cpx
21	-362.5	85.8,m	1.2	-	-	-	0.4	6.0	0.2	5.6	0.8	2.5	ol,pl±cpx
22	-363.9	87.4,m	0.4	-	-	-	0.2	7.0	-	4.6	0.4	2.5	ol,pl,cpx
23	-367.3	99.0,c	1.0	-	-	-	-	0.01	-	0.01	-	2.5	ol,pl±cpx
24	-370.9	99.2,c	0.4	-	-	-	-	0.4	-	0.4	-	2	ol,pl±cpx
25	-372.6	99.8,c	0.2	-	-	-	-	0.01	-	0.01	-	1.5	ol,pl±cpx
26	-376.1	84.8,m	2.0	-	-	-	-	6.6	-	6.6	-	2	ol,pl±cpx
27	-379.5	93.0,m	0.6	0.2	-	-	0.4	3.6	-	2.2	-	2.5	ol,pl,cpx
28	-379.8	92.2,m	0.8	-	-	-	0.4	3.6	-	3.0	-	3	ol,pl,cpx
29	-381.4	75.2,m	21.2	-	-	-	-	2.0	-	1.6	-	2	ol,pl,cpx
30	-383.4	85.0,m	1.8	1.2	-	-	1.8	5.8	-	4.4	-	2.5	ol,pl,cpx
31	-387.6	73.8,m	23.0	-	-	-	0.2	2.2	-	0.8	-	3	ol,pl,cpx
32	-388.2	82.8,m	16.2	-	-	-	-	0.6	-	0.4	-	3	ol,pl±cpx
34	-391.5	79.0,m	5.8	-	-	-	-	6.2	-	8.6	0.4	2.5	ol,pl±cpx
35	-392.0	93.2,c	6.0	-	-	-	-	0.4	-	0.4	-	2.5	ol,pl±cpx
36	-394.4	87.8,c	11.2	-	-	-	-	0.6	-	0.6	-	2.5	ol,pl±cpx
37	-395.8	97.2,m	2.0	-	-	-	-	-	-	-	0.8	2	ol,pl,cpx
38	-398.5	94.8,m	3.4	1.0	-	-	-	0.8	-	-	-	2.5	ol,pl,cpx
39	-403.8	95.8,c	3.0	0.2	-	-	0.01	0.4	-	0.6	-	2.5	ol,pl,cpx
40	-407.6	95.6,c	2.6	1.0	-	-	0.01	0.4	-	0.4	-	2.5	ol,pl,cpx
41	-408.8	96.8,m	0.6	1.2	-	-	0.2	0.6	0.2	0.4	-	2.5	ol,pl±cpx
44	-411.3	98.0,c	1.0	0.4	-	-	0.2	0.2	0.2	0.2	-	2	ol,pl±cpx
45	-412.3	98.4,m	0.2	1.4	-	-	-	-	-	-	-	2	ol,pl±cpx
46	-413.6	89.4,m	0.2	0.2	-	-	2.4	4.6	1.4	1.8	-	2	ol,pl,cpx
47	-418.9	87.0,m	4.0	0.4	-	-	1.8	3.0	1.6	2.2	-	2.5	ol,pl,cpx
48	-422.7	93.6,m	2.0	0.4	-	-	0.8	2.0	-	1.2	-	2.5	ol,pl,cpx
49	-426.2	83.6,m	1.4	1.0	-	-	-	7.0	-	7.0	-	2.5	ol,pl±cpx
50	-429.7	93.8,m	4.2	1.0	-	-	0.01	0.4	0.01	0.6	-	2.5	ol,pl±cpx
51	-433.9	97.2,c	1.2	0.2	-	-	0.2	0.8	-	0.4	-	2.5	ol,pl±cpx
52	-439.0	58.4,m	14.0	0.8	-	-	-	13.8	-	13.0	-	2.2	ol,pl±cpx

Table 8. (cont.)

Unit	Depth	Gmass	ol		opx		plag		cpx		opq	A.I.	Crystallization
	(m)	(%, c/m)	ph	mph	ph	mph	ph	mph	ph	mph	mph	(1-5)	Sequence
53	-440.4	82.4,m	11.4	-	-	-	-	2.8	-	3.4	-	2.2	ol,cpx±pl
54	-443.8	90.6,c	0.4	-	-	-	-	6.0	-	2.8	0.2	2	ol,pl,cpx
55	-445.8	86.6,c	0.4	0.4	-	-	1.8	4.6	1.4	4.8	-	2	ol,pl±cpx
56	-448.8	75.6,c	4.2	-	-	-	0.4	11.2	0.2	8.0	0.4	2.5	ol,pl,cpx
57	-453.2	75.2,c	4.0	-	-	-	1.6	10.2	1.2	7.8	-	2.5	ol,pl,cpx
59	-456.2	93.0,c	1.4	-	0.01	-	2.6	1.0	0.8	-	1.2	2.5	ol,opx±pl±cpx
60	-464.5	83.6,c	1.6	-	0.01	-	8.0	3.0	1.0	2.8	-	3	ol,opx±pl±cpx
61	-469.4	64.6,m	3.2	-	0.2	-	13.4	5.2	5.8	6.2	1.4	2.5	ol,opx,pl,cpx
62	-476.4	65.0,m	1.6	-	1.8	-	12.6	6.8	5.8	4.4	2.0	1	ol,opx,pl,cpx
63	-482.1	72.2,m	3.0	-	0.4	-	9.6	6.6	2.8	3.0	2.4	2.5	ol,opx±pl,cpx
64	-493.6	54.4,m	9.2	-	4.0	-	15.0	5.8	4.0	6.2	1.4	2.5	ol,opx,pl,cpx
65	-495.8	84.8,m	3.8	-	-	-	1.8	7.0	-	2.6	-	2.5	ol,pl,cpx
66	-506.9	80.4,m	1.4	-	-	-	0.4	10.6	-	5.6	1.6	2.8	ol,pl,cpx
67	-511.0	77.4,m	7.2	-	0.2	-	0.2	10.8	-	3.8	0.4	2.5	ol,opx,pl,cpx
68	-514.3	78.8,c	5.0	-	2.4	-	0.2	8.4	-	4.2	1.0	2.5	ol,opx,pl,cpx
69	-521.8	97.4,c	0.2	-	-	-	-	1.8	-	0.6	-	3	ol,pl,cpx
70	-526.0	91.0,c	3.2	1.0	-	-	0.2	2.0	-	1.2	1.4	2.5	ol,pl,cpx
71	-526.6	94.2,c	1.4	1.6	-	-	-	1.8	-	0.6	0.4	2.5	ol,pl,cpx
72	-533.8	99.0,c	0.1	-	-	0.1	-	0.01	0.2	0.6	-	1.5	ol,opx,pl±cpx
73	-535.4	96.6,c	1.0	0.4	-	-	0.2	1.2	-	0.6	-	2.5	ol,pl,cpx
74	-537.9	91.8,c	0.6	0.2	0.01	-	-	5.4	0.2	1.8	-	2.5	ol,opx±pl,cpx
75	-545.1	95.6,c	-	-	-	1.2	0.01	-	-	0.4	2.8	2.5	ol,opx±pl±cpx
76	-550.3	90.4,m	3.8	-	-	-	-	3.6	-	2.2	-	2.5	ol,pl,cpx
81	-556.4	96.4,c	2.2	0.4	-	-	-	0.8	-	0.2	-	2	ol,pl,cpx
82	-558.7	90.8,m	0.4	0.2	-	-	0.2	5.6	0.01	2.8	-	2.5	ol,pl,cpx
83	-562.0	96.6,?	1.8	-	-	-	-	1.0	-	0.6	-	3	ol,pl,cpx
85	-564.9	86.2,m	10.4	-	-	-	-	2.8	-	0.4	-	4	ol,pl,cpx
86	-565.8	87.0,m	6.6	-	2.4	0.8	0.01	0.2	1.0	0.8	0.6	4	-
88	-569.4	72.2,m	13.6	-	-	-	2.6	8.4	-	3.0	0.2	4	ol,pl,cpx
91	-573.7	79.4,m	4.2	-	-	-	0.2	9.2	0.6	4.8	1.6	3.5	ol,pl±cpx
92	-581.9	66.4,m	33.0	-	0.01	-	0.01	0.4	0.01	0.01	0.2	3.2	ol,opx±pl±cpx
93	-586.4	97.8,m	0.6	-	-	-	0.01	1.6	-	0.01	-	3	ol,pl,cpx
94	-590.5	93.2,m	4.2	-	-	-	-	1.6	-	1.0	-	4	ol,pl,cpx
95	-593.7	93.6,m	1.8	-	-	-	-	3.0	-	1.6	-	4	ol,pl,cpx
96	-296.0	93.0,m	2.0	-	-	-	0.2	3.2	-	1.6	-	4	ol,pl,cpx
97	-597.7	74.2,c	22.2	-	-	-	1.8	0.6	1.2	-	-	4	ol,pl,cpx
98	-600.3	97.8,m	1.8	-	-	-	-	0.4	-	0.01	-	4	ol,pl,cpx
99	-604.6	69.4,c	30.6	-	-	-	-	-	-	-	-	5	ol,cpx
100	-606.3	77.6,m	0.4	-	-	-	2.6	10.4	0.01	9.0	-	4	ol,pl,cpx
101	-622.4	89.6,m	2.2	-	-	-	0.2	5.4	-	2.6	-	4	ol,pl,cpx
102	-625.5	76.2,m	8.2	-	-	-	1.2	9.4	-	5.0	-	4	ol,pl,cpx
103	-627.8	96.8,m	1.4	-	-	-	0.2	1.0	-	0.6	-	4	ol,pl,cpx

A.I. = alteration index, ranging from 1-5, increasing with extent of alteration (details in text).
Groundmass texture: c = cryptocrystalline, m = microcrystalline.
ph = phenocrysts, opq = opaque phases; mph, ol, opx, plag, cpx as in Table 6.

Cored Section Petrography

Phenocrysts of olivine, plagioclase, and clinopyroxene are all commonly present in the KSDP core, while orthopyroxene phenocrysts are rare compared to the rotary-drilled section (14% vs. 61.5%). Olivine is usually the most abundant phenocryst phase, and textural relationships indicate that it was the first to crystallize. Many olivine phenocrysts exhibit skeletal growth, suggesting they formed rapidly. In addition, many flows contain numerous olivine xenocrysts that were oxidized by baking. Olivine is altered to varying degrees in most units. In the highly altered flows at the bottom of the cored section (550 - 630 mbsl), olivine is almost completely replaced by iddingsite.

In addition to its relative rarity in the cored section, orthopyroxene is unevenly distributed with depth. It is present as a xenocryst in the first three cored units (303.8 – 308.9 mbsl), and as a phenocryst in three other flows near the top (332.4 - 336.2 mbsl) of the cored section (Table 4). Orthopyroxene is absent in the section until 456.2 mbsl and below, but is a significant phase (≥0.2% phenocrysts) in only 19% of these flows. Where present, orthopyroxene is smaller than in the rotary-drilled section (0.5 - 6 mm vs. up to 10 mm), almost always contains olivine inclusions, and is commonly surrounded by a thin rim (~0.1 mm) of clinopyroxene microphenocrysts and/or contains clinopyroxene lamellae. This orthopyroxene-clinopyroxene reaction relationship was observed in only one thin section from the rotary-drilled portion of the hole (215 mbsl).

Plagioclase is common in the KSDP core, second in abundance only to olivine. This phase is present in variable amounts (0-14%) as unaltered phenocrysts and microphenocrysts, and is always present in the groundmass. Plagioclase phenocrysts and/or microphenocrysts occur in clusters with clinopyroxene of the same size, and the

two minerals occur in similar abundances (Table 8), indicating that these two phases crystallized almost simultaneously.

The presence of clinopyroxene phenocrysts in 27 of 91 basalt units is the most striking petrographic feature of the cored section, because of their absence in the rotary-drilled section. In addition, microphenocrysts of clinopyroxene are more abundant in the cored section. Many clinopyroxene phenocrysts and microphenocrysts throughout the section exhibit sector zoning. All clinopyroxene phenocrysts are euhedral, there is no indication of clinopyroxene dissolution in any of the core thin sections.

The dominant crystallization sequence in KSDP cored lavas is olivine± orthopyroxene + plagioclase + clinopyroxene. Although this crystallization sequence is the same as that determined for Ko'olau lavas from previous studies (Frey et al., 1994), the relative pyroxene abundances are much different. The presence of orthopyroxene and the absence of clinopyroxene phenocrysts is characteristic of typical Ko'olau rocks (Winchell, 1947), so the greater abundance of clinopyroxene vs. orthopyroxene phenocrysts and the common reaction relationship between these two phases in KSDP lavas indicate geochemical differences from subaerially exposed Ko'olau flows. The presence of clinopyroxene phenocrysts and greater abundance of clinopyroxene microphenocrysts in KSDP cored section lavas indicate earlier crystallization of this phase than in typical Ko'olau lavas. However, in the vast majority of KSDP lavas, clinopyroxene crystallization still follows that of plagioclase, although more closely. Rare sections have more clinopyroxene than plagioclase (Table 8), as observed in Kilauea lavas (Helz & Thornber, 1987).

Lithologic unit 86 contains a matrix of altered and opaque material. Large opaque phenocrysts are completely altered. In order of abundance, olivine, orthopyroxene, clinopyroxene, and plagioclase occur as both fresh and highly altered grains. Most of these grains are rounded both in thin section and hand specimen, indicating mechanical weathering in addition to the high level of chemical weathering (alteration) observed in thin section. For these reasons, this unit was classified as a fluvial sandstone.

Geochronology

New Ar-Ar plateau ages for KSDP Units 14, 19, and 66 all fall within 2.90 ±0.23 Ma (Table 6). The different age determinations (plateau, normal isochron, and inverse isochron ages) all overlap within analytical error, providing independent confirmation of these ages for the KSDP section. Thus, the age progression with depth is unknown because the rate of emplacement for most of the KSDP section exceeds the resolution of even the Ar-Ar dating technique. The ages are significantly older than those previously determined by K-Ar methods (1.8 – 2.6 Ma; Doell & Dalrymple, 1973; Lanphere & Dalrymple, 1980). KSDP lava flow ages indicate eruption in the Gauss normal period, which is consistent with a paleomagnetic study of the core (Carey, 2001). We suspect that the original Ko'olau ages are underestimates limited by their K-Ar dating technique, although KSDP core samples are deeper than any surface samples and are therefore expected to be older. It is most likely that all of the subaerially exposed lavas sampled and dated in these studies have very early Matuyama ages (2.4 – 2.6 Ma), and that their published ages are younger as a result of K loss due to postmagmatic alteration. The overall freshness of KSDP compared to surface Ko'olau lavas, the strict criteria used to

select unaltered KSDP samples, and internal checks of age reliability using the Ar-Ar technique gives us greater confidence in these new ages.

Ko'olau Geochemistry

Previous studies of Ko'olau basalts (Wentworth and Winchell 1947; Stille et al. 1983; Roden et al. 1984, 1994; Budahn and Schmitt 1985; Frey et al. 1994; Eiler et al. 1996; Lassiter & Hauri, 1998) showed that these lavas represent a geochemical and isotopic end member among Hawaiian shield tholeiites. Ko'olau lavas have the highest observed SiO_2, Al_2O_3, and Na_2O and the lowest observed Fe_2O_3 and CaO at a given MgO, leading to the correspondingly highest values of Al_2O_3/CaO and Na_2O/CaO (Frey et al., 1994). The high Sr, La, Zr, and relatively low Nb in Ko'olau lavas are responsible for their high ratios of Zr/Nb, Sr/Nb, and La/Nb among Hawaiian tholeiites (Frey et al., 1994). In addition, Ko'olau lavas have near bulk-earth $^{87}Sr/^{86}Sr$ and $^{143}Nd/^{144}Nd$ (and relatively low Pb isototope ratios), which define an end member within the Hawaiian isotopic array (Roden et al., 1984). KSDP whole-rock major and trace element analyses as well as major element glass analyses are compared to those of previous Ko'olau studies to better determine the geochemical evolution of the volcano.

Whole-Rock Postmagmatic Alteration Effects

Subaerial weathering in the tropical environment of the Hawaiian Islands generally causes severe loss of K_2O in basalts, while P_2O_5 remains relatively unaffected (e.g., Feigenson et al. 1983; Lipman et al. 1990; Frey et al. 1994). As a result, surface alteration lowers the original K_2O/P_2O_5 ratio. Frey et al. (1994) have shown that alteration may also result in lower SiO_2 and CaO, and higher Fe_2O_3, Al_2O_3, and TiO_2

abundances in Ko'olau rocks. In order to gain an unambiguous understanding of KSDP lavas with respect to previous studies of Ko'olau and other Hawaiian shields, altered samples were removed from both our own data set and those from previous studies. The criteria for removal are explained below.

Most KSDP rotary-drilled samples (72%) have lower than magmatic K_2O/P_2O_5 values (1.2 – 2.0 based on criteria discussed below) and/or loss on ignition (LOI) values >0.5 wt%, indicating alteration. In contrast, most of the cored lavas selected for analysis (74%) are unaltered according to these criteria (Tables 3 & 8). Petrographic examination of rock cuttings picked on the basis of their relatively unaltered appearance revealed a highly variable extent of alteration. The extent of KSDP core alteration was independently evaluated by petrographic examination of thin sections. A petrographic alteration index (AI) was created to rate the level of alteration. Index values range from 1-5, with 1 – representing unaltered rock, 2 – some weak alteration with iddingsite rims on olivine, 3 – internal olivine alteration, 4 – intense olivine alteration with some matrix alteration, and 5 – plagioclase alteration and abundant secondary minerals such as calcite, zeolites, and/or clays (particularly in vesicles). Most KSDP basalts have AI values from 1.5 – 3 (Table 8).

KSDP samples are considered altered if they meet two of the following three criteria: AI values >3, >0.5 wt% LOI, and K_2O/P_2O_5 <1.2 (Table 3, Fig. 7). Of the first 74 core units analyzed, 67 are unaltered according to these criteria and confirm our prediction that the subsurface shield-stage lavas from the leeward portion of the Ko'olau shield have been subject to little weathering. However, the deeper units (81-103; 556.4 - 627.8 mbsl) are all significantly altered, but to varying degrees (Table 3, Fig. 7). The

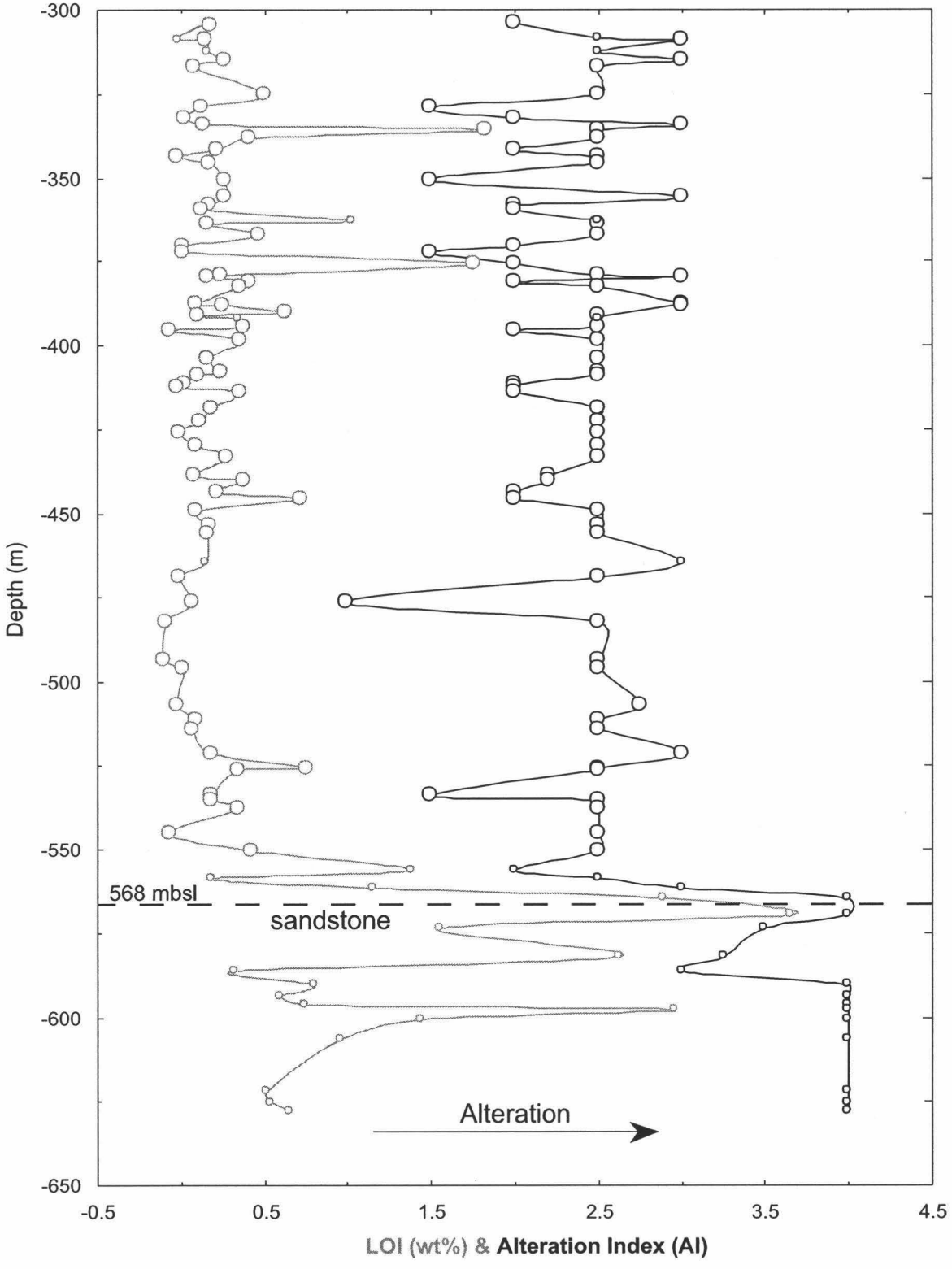

Fig. 7. KSDP core alteration vs. depth. Smaller symbols indicate K_2O/P_2O_5 <1.2. Few samples are altered above 550 mbsl, indicating that the subsurface lavas on the leeward side of Ko'olau volcano still contain fresh material. Deep alteration is primarily the result of hydration by a paleostream at 568 mbsl. Note that all samples with AI >3 have K_2O/P_2O_5 <1.2 and high average LOI values. Unit 99 (604.6 mbsl) has an AI of 5, but was not analyzed for LOI.

presence of fluvially deposited sedimentary material suggests that these 23 deepest units may have been altered by a surface stream or groundwater hydration. The high LOI values for most of these flows indicate significant hydration of the samples, and support such an interpretation.

Rather than discard the potentially important geochemical indicators from the rotary-drilled and deeply cored portions of the KSDP, we evaluated the effects of alteration on the distinctive major element signatures and LOI values of Ko'olau lavas (Fig. 8). Previous studies have shown that alteration causes loss of SiO_2 and residual gain of Al_2O_3 in Ko'olau and other Hawaiian lavas (Frey et al., 1994, Lipman et al., 1990). In a plot of K_2O/P_2O_5 vs. SiO_2/Al_2O_3, the large relative loss of K_2O is still the most obvious indicator, but SiO_2 loss and residual gain of Al_2O_3 with increasing alteration drive SiO_2/Al_2O_3 values downward as well.

Ko'olau lavas are known to have distinctively high Al_2O_3/CaO and Na_2O/CaO values. Surface Ko'olau lavas from Makapu'u Head and the Wheeler Air Force Base (WAFB) core show slight increases in Al_2O_3/CaO with decreasing K_2O/P_2O_5, but all samples from the KSDP (save the most highly altered flow, Unit #88, with the highest LOI) fall within the geochemical range of Al_2O_3/CaO values of unaltered KSDP flows (Fig. 8). Postmagmatic alteration does not significantly modify Al_2O_3/CaO values in the vast majority of Ko'olau lavas. KSDP Na_2O/CaO is not modified by alteration; all samples with $K_2O/P_2O_5 < 1.2$ have Na_2O/CaO values within the range of unaltered rock, regardless of the extent of alteration. However, since there are numerous samples from the cored section with $K_2O/P_2O_5 > 1.2$, the only altered samples shown in subsequent geochemical diagrams (e.g., Fig. 9) are from the rotary-drilled section due to the lack of

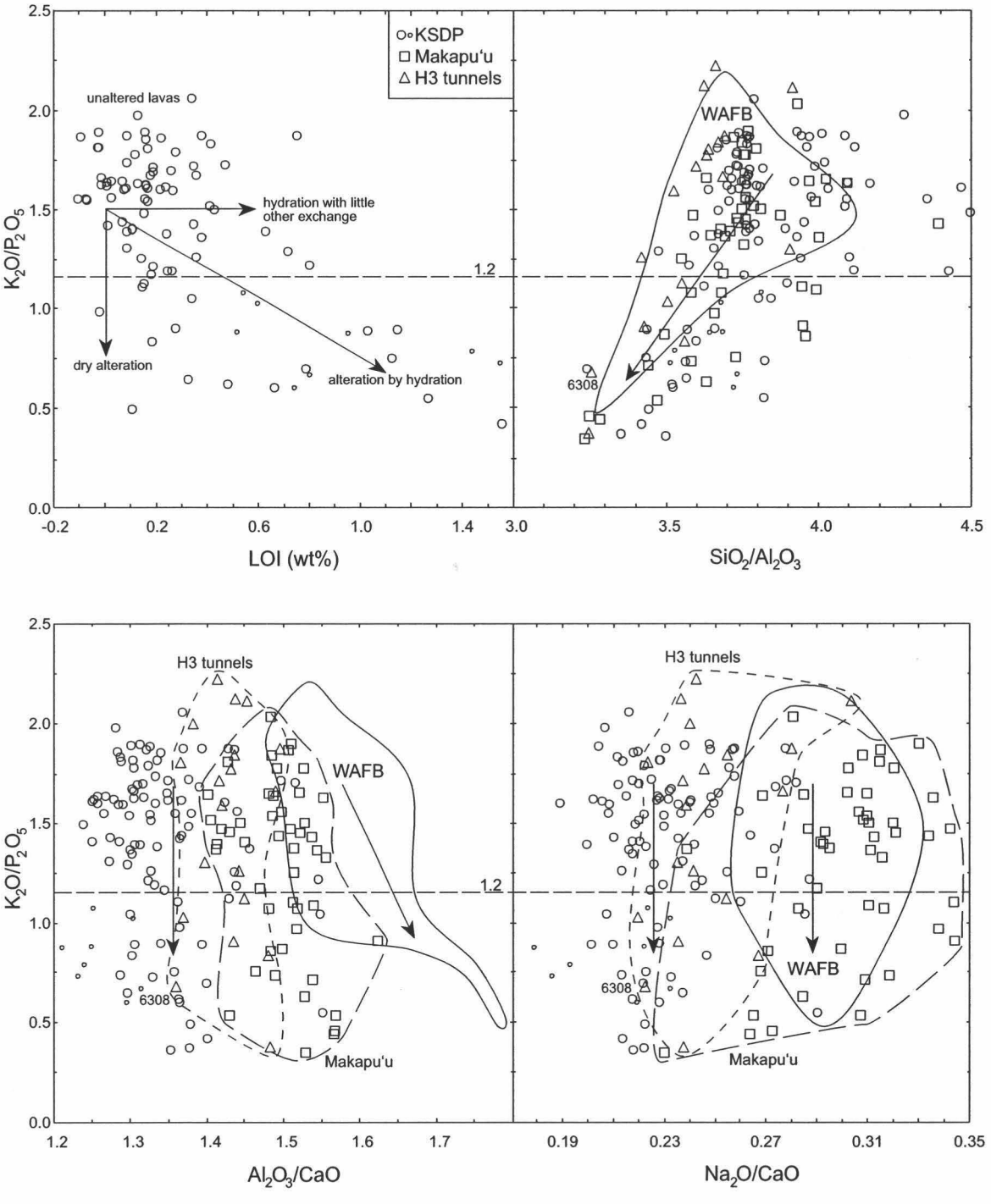

Fig. 8. Whole-rock alteration effects on shield-stage Ko'olau lavas. Small symbols have AI >3. In the upper left panel, 10 rotary section lavas could not be plotted due to an insufficient amount of sample material for LOI analysis. Six of these samples have K_2O/P_2O_5 <1.2. Wheeler Air Force Base (WAFB) fields contain data from Takeguchi and Takahashi (unpub.), and unlabeled arrows indicate direction of alteration. While K_2O/P_2O_5 generally decreases and LOI increases with increasing alteration, other geochemical characteristics are also affected. Loss of SiO_2 and residual gain of Al_2O_3 due to alteration causes a decrease in the the ratio of these two elements. Of the distinctive geochemical ratios used to separate typical Ko'olau and KSDP lavas, only WAFB Al_2O_3/CaO is significantly affected by alteration, increasing due to residual gain of Al_2O_3 from loss of other elements.

data representing this portion of the KSDP. There are a sufficient number of unaltered lavas from the H3 tunnel (68% of published analyses) and Makapu'u (65% of published analyses) studies for comparison with the KSDP, so samples with K_2O/P_2O_5 <1.2 have been removed from these suites as well.

KSDP Whole-Rock Major Element Composition

Like most Hawaiian tholeiites from a given volcano, KSDP lavas have a wide range in MgO content (6.6-21.7 wt%; Table 3), and define generally linear trends for major element oxides vs. MgO above 7.5 wt% MgO (Fig. 9). These features are indicative of olivine controlled crystal fractionation and olivine accumulation (Wright & Fiske, 1971). KSDP lavas define subhorizontal trends for Al_2O_3/CaO and Na_2O/CaO independent of olivine fractionation, with the majority of data points neither increasing nor decreasing at low MgO due to the competing effects of plagioclase and clinopyroxene crystallization. Exceptions to this trend are rare KSDP samples with high Al_2O_3/CaO and Na_2O/CaO, which will be discussed below.

The KSDP whole-rock major element data are distinct from typical Ko'olau compositions described above and represented by Makapu'u Head (Frey et al., 1994) and WAFB core (Takeguchi & Takahashi, in review.). Most KSDP samples have lower Na_2O and higher CaO at a given MgO than typical Ko'olau lavas, and the abundances of these elements are similar to those of Mauna Loa (Fig. 9). The KSDP lavas have relatively high SiO_2 and Al_2O_3 abundances compared to typical Hawaiian tholeiites (like typical Ko'olau rocks). Compared to typical Ko'olau lavas, many of the rotary-drilled samples fall below the SiO_2 vs. MgO array. These samples are altered (low K_2O/P_2O_5),

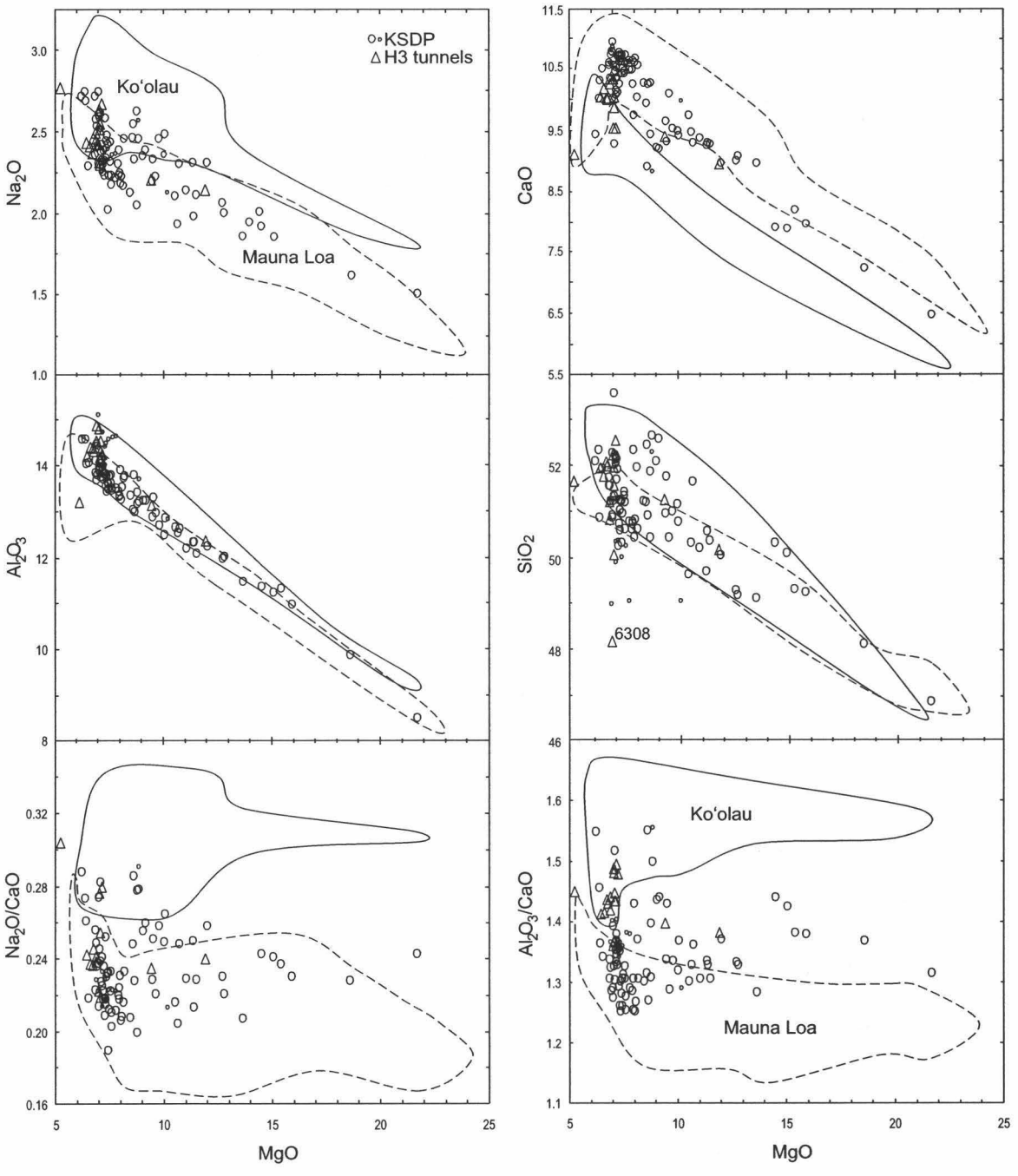

Fig. 9. Whole-rock MgO variation diagrams. Symbols same as in Figure 7, except small KSDP symbols have $K_2O/P_2O_5<1.2$. The solid border encloses typical Ko'olau lavas from Makapu'u and the WAFB core (Takeguchi and Takahashi, unpub.). The dashed border encloses Mauna Loa analyses from Rhodes (unpub.). All analyses except WAFB are from the same lab (UMass), thereby avoiding interlaboratory bias in this comparison. Note that typical Ko'olau and Mauna Loa lavas are distinct for Na_2O and CaO, and that KSDP rocks are more similar to those of Mauna Loa, for these but not all oxides. H3 tunnel samples have compositions between those of typical Ko'olau and Mauna Loa. See text for discussion.

and appear to have lost significant SiO_2. Likewise, the Al_2O_3 contents of these samples are high at a given MgO as a result of residual Al_2O_3 gain from alteration (Table 3, Figs. 8 & 9). Mauna Loa lavas also have relatively high Al_2O_3 and SiO_2 values (Fig. 9). In general, KSDP samples plot between the fields defined for these two volcanoes (Fig. 9). The H3 tunnel samples plot with KSDP data, but most have low MgO abundances and are located where Ko'olau and Mauna Loa fields overlap. This observed overlap of major element compositions is not unexpected, as Mauna Loa rocks bear a geochemical (Frey et al., 1994) and petrologic resemblance (orthopyroxene present) to subaerially exposed Ko'olau lavas.

Plots of Al_2O_3/CaO and Na_2O/CaO vs. MgO illustrate the compositional differences between lavas from Mauna Loa and Ko'olau volcanoes (Fig. 9). Typical Ko'olau lavas have Al_2O_3/CaO >1.45 and Na_2O/CaO >0.26, although several Makapu'u lavas have lower Al_2O_3/CaO due to significant plagioclase fractionation with little to no clinopyroxene crystallization. Only one unaltered sample from the Makapu'u section (KOO22; Frey et al., 1994) has a geochemical composition outside of both the Al_2O_3/CaO and Na_2O/CaO fields of surface Ko'olau lavas. Typical Mauna Loa lavas have distinctly lower Al_2O_3/CaO and Na_2O/CaO ratios of ~1.28 and ~0.21, respectively. Only low-MgO (<5.8 wt%) Mauna Loa lavas fractionate sufficient clinopyroxene and/or plagioclase to reach Na_2O/CaO values >0.26.

The vast majority of unaltered KSDP samples have Al_2O_3/CaO and Na_2O/CaO values in the upper Mauna Loa range. However, all of the KSDP shield-stage lavas from above 182 mbsl as well as the flows at 209 and 215 mbsl consistently plot within the Ko'olau fields (Fig. 9). The geochemistry of KSDP lavas is otherwise relatively

constant, although three consecutive flows from deep in the cored section (Units 67 - 69 from 511 - 522 mbsl) have transitional compositions (Na_2O/CaO 0.26 – 0.28, but Al_2O_3/CaO 1.37 – 1.39). A wide range of geochemical variability among flow units is also observed in the H3 tunnel section, despite their limited MgO range. Like KSDP lavas, the compositions of these flows are transitional between Ko'olau and Mauna Loa, and they span the Al_2O_3/CaO and Na_2O/CaO boundaries.

KSDP Whole-Rock Trace Element Composition

KSDP trace element analyses (Table 4) from the cored section revealed unexpected results. When lavas that have experienced similar extents of crystal fractionation are compared (Fig. 10), incompatible element abundances illustrate differences between previously published Ko'olau and new KSDP lava compositions. Incompatible trace element compositions of KSDP flows are intermediate between those of typical Ko'olau and Mauna Loa rocks as seen for major elements, but there are additional complexities in the data. KSDP major element compositions strongly resemble Mauna Loa, but the normalized incompatible trace element patterns defined by individual KSDP samples are more intermediate between surface Ko'olau and Mauna Loa (Fig.10). With increasing incompatibility, KSDP lavas exhibit a progressively wider range of values. KSDP lavas can have Ko'olau-like, intermediate, or Mauna Loa-like compositions depending on the incompatible element examined (e.g. Unit 75). The similar concentrations of Y in all three data suites are consistent with buffering of this element by residual garnet in the melting region.

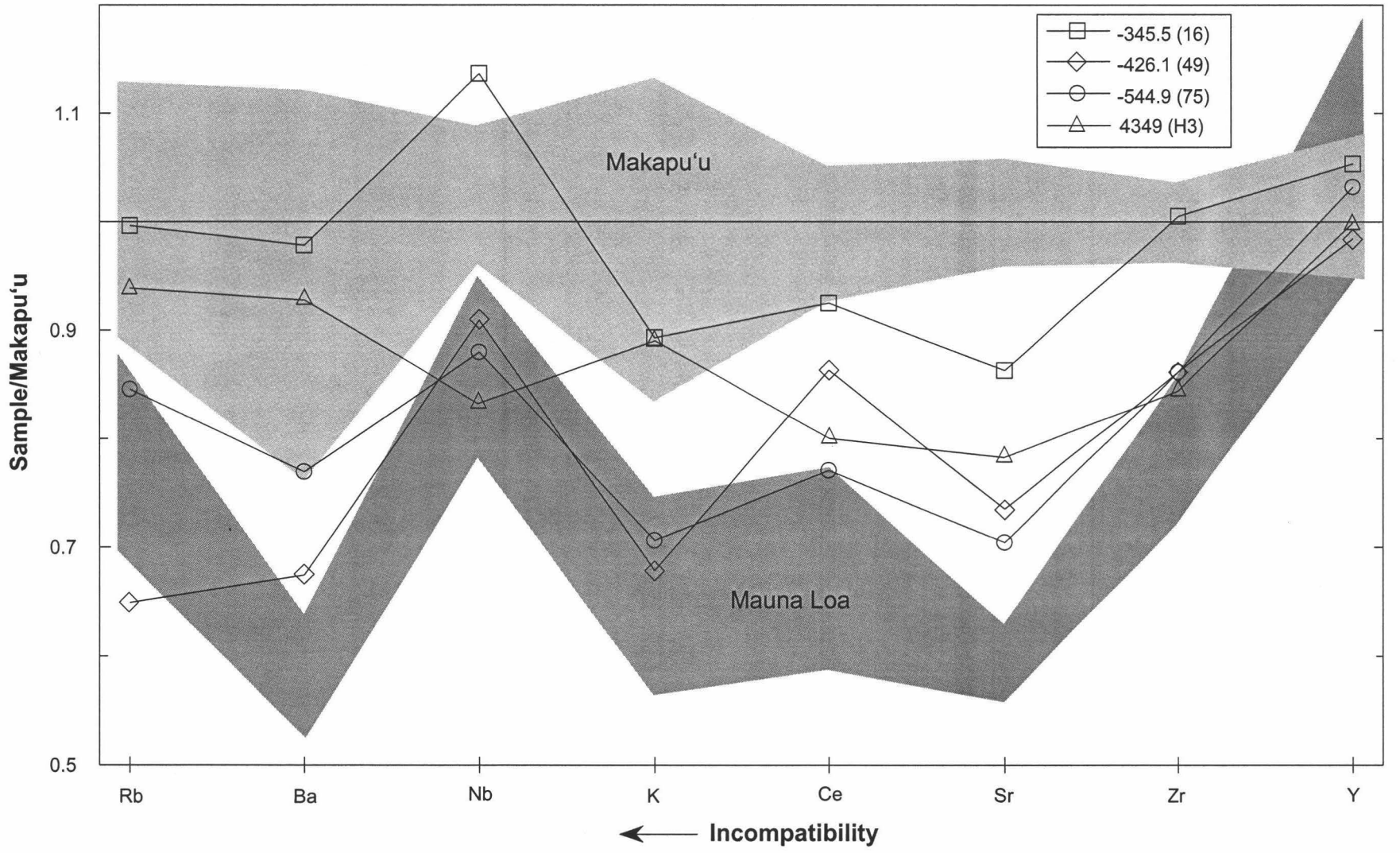

Fig. 10. Selected KSDP and H3 trace element patterns vs. typical Ko'olau (Makapu'u; Frey et al., 1994) and Mauna Loa (Rhodes, unpub.) ranges. All samples have 7.2-7.6 wt% MgO and have been normalized to the average Makapu'u composition for comparative purposes. Fields are defined by at least five samples.

Typical Ko'olau lavas have high abundances of incompatible trace elements, although KSDP Unit 16 has the highest Nb value. In general, Unit 16 resembles Makapu'u compositions more than any other KSDP sample, particularly in terms of the highly incompatible elements. The intermediate Sr content of KSDP rocks is the only signature completely distinct from both the Makapu'u section and Mauna Loa, although other similarly incompatible elements like Ce and Zr also have intermediate abundances that show little overlap with either data field (Fig. 10). H3 lavas have intermediate abundances of these moderately incompatible elements as well, regardless of their Ko'olau or KSDP-like major element geochemistry (determined by Al_2O_3/CaO and Na_2O/CaO values). H3 sample 4349 has a Mauna Loa-like Nb concentration, a negative Nb anomaly typical of surface Ko'olau lavas, high Al_2O_3/CaO and Na_2O/CaO values, indicating its transitional nature.

Na_2O loss in Glasses from Ko'olau Volcano

Volcanic glass sampled from variably baked flow and intraflow contacts was common beneath baked soil, and showed signs of surface weathering. Despite the extensive alteration of whole-rock samples near the bottom of the section, unaltered glass was recovered in this region, providing a less compromised geochemical view of KSDP material to even greater depths. A majority of the 65 KSDP glassy samples collected (~55%) were determined by binocular microscopic examination to have an altered appearance (waxy, dull, reddish color from oxidation, or strongly opaque). These glasses were not analyzed. Nine of the glassy samples that appeared to be fresh produced heterogeneous major element concentrations and totals. Nineteen of the glasses yielded

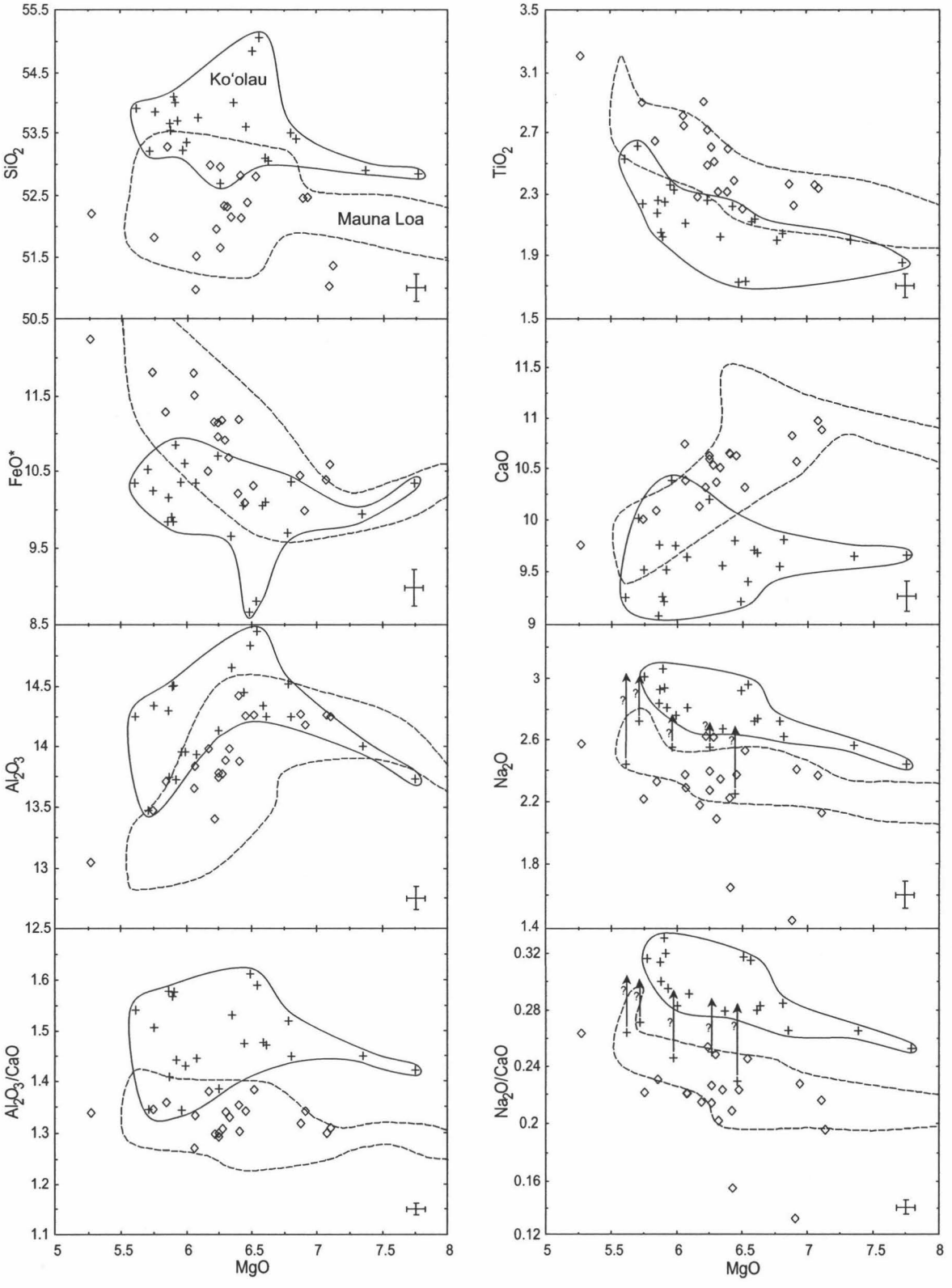

Figure 11. MgO variation diagrams for KSDP glasses, compared to Ko'olau (solid field, crosses) and Mauna Loa (dashed field). See text for data sources. Arrows with ?'s indicate Ko'olau glasses that may have lost Na_2O. Error bars in lower right corner represent absolute analytical error.

uniform major element abundances, acceptable totals (98.5 – 100.2 wt%), and K_2O/P_2O_5 >1.5, suggesting that they are unaltered. However, two of these samples have unusually low Na_2O (<2 wt%; Table 5), which may be caused by some process other than surface weathering. There are also five subaerial Ko'olau flow and dike glass samples (Garcia, unpub. data) with relatively low Na_2O contents (Fig. 11). The low Na_2O of these few Ko'olau and KSDP samples produces an uncharacteristically wide range of abundances vs. MgO compared to other oxides in the two data suites, indicating that Na_2O is the only element significantly affected by modification. A post-analysis microscopic examination of KSDP glass analyses revealed that only glass samples with translucent brown edges produced reasonably high Na_2O abundances as well as uniform totals and abundances for other oxides. Our visual selection criteria should have been even more discriminating, removing opaque samples regardless of their luster.

This phenomenon of Na_2O loss in Hawaiian lavas has been observed in Ko'olau (Frey et al., 1994) as well as Mauna Kea glasses (Garcia, 1996), and has been suggested by the former to be alkali metal modification by incipient hydration. Palagonitization studies of basaltic glass have revealed that significant amounts of Na_2O can be removed from the glass quite rapidly during alteration (Furnes, 1975; Jakobsson, 1972). Despite our efforts to minimize Na_2O migration, the fact that Na_2O is the only element affected points to its mobile nature. Migration of this element away from the analyzed area even under a low-intensity and diffuse electron microprobe beam is another possible explanation for its low values.

KSDP Major Element Glass Composition

Flow contact and intraflow glasses from the KSDP core have a limited MgO range (5.3 – 7.1 wt%; Table 5). The highest SiO_2 content of a KSDP glass is 53.3 wt%, with a wide range (up to 2 wt%) at a given MgO (Fig. 11). The variation trends for KSDP glasses decrease for both CaO and Al_2O_3 with decreasing MgO, indicating crystallization of plagioclase and clinopyroxene. Like the whole-rock data, and unlike the surface Ko'olau glass data, KSDP glasses define near-horizontal Al_2O_3/CaO trends, suggesting simultaneous crystallization of both of these phases. This interpretation is supported by our petrographic observations of higher clinopyroxene abundances in KSDP than surface Ko'olau lavas.

Fresh volcanic glass is usually a better indicator of magmatic composition than whole-rock data, because mineral accumulation modifies the sample composition. The KSDP major element glass compositions show similar intervolcano trends as the whole-rock data for most oxides vs. MgO (Fig. 11). CaO, Al_2O_3/CaO, and Na_2O/CaO vs. MgO retain their distinctive relationships inferred from whole-rock analyses. However, TiO_2 and SiO_2 vs. MgO data for Ko'olau and KSDP glasses are more distinct than for whole-rock data. KSDP glass samples have Mauna Loa-like compositions in all of these plots (Fig. 11). The slight offset between Mauna Loa and KSDP whole-rock data is not as evident in glass data, probably due to the moderate to low MgO of KSDP glass samples. KSDP and Mauna Loa glasses have similar mean Al_2O_3/CaO values, 1.34 and 1.31 respectively, and identical mean Na_2O/CaO ratios of 0.23. KSDP whole-rock ratios are identical to their glass ratios, while a few Mauna Loa rocks have low Al_2O_3/CaO and Na_2O/CaO values that lower their averages slightly to 1.28 and 0.21. Although CaO and

Al_2O_3/CaO fields for Ko'olau and Mauna Loa overlap at more evolved glass compositions (<6.4 wt% MgO), the vast majority of KSDP glasses consistently fall within the Mauna Loa fields.

DISCUSSION

Geochemical Stratigraphy

The geochemical contrasts between KSDP and typical Ko'olau indicate that shield-stage growth of Ko'olau volcano contained at least two geochemical substages (Fig. 12). Ratios of Al_2O_3/CaO and Na_2O/CaO for KSDP lavas are Mauna Loa-like below 215 mbsl, variable from 215 – 182 mbsl, and Ko'olau-like above 182 mbsl. Representative Sr abundances from the KSDP, H3, and Makapu'u data suites show the same type of behavior, with Mauna Loa lavas containing distinctly low Sr at a given MgO (Fig. 10).

KSDP lavas show variations in composition between successive samples from the rotary-drilled section. Four analyses from 209 – 218 mbsl alternate between typical Ko'olau and Mauna Loa-like Al_2O_3/CaO and Na_2O/CaO ratio values. Unfortunately, the zone of no recovery (89 – 173 mbsl) and altered nature of rock cuttings between 182 and 209 mbsl prevented precise characterization of the geochemistry and stratigraphy of the transitional interval beneath Kalihi. However, flows sampled from the H3 tunnels have Al_2O_3/CaO and Na_2O/CaO ranges similar to the few transitional KSDP flows, providing both independent confirmation and greater sampling resolution of the geochemically transitional interval. While the two shallowest H3 tunnel flows have high Al_2O_3/CaO and

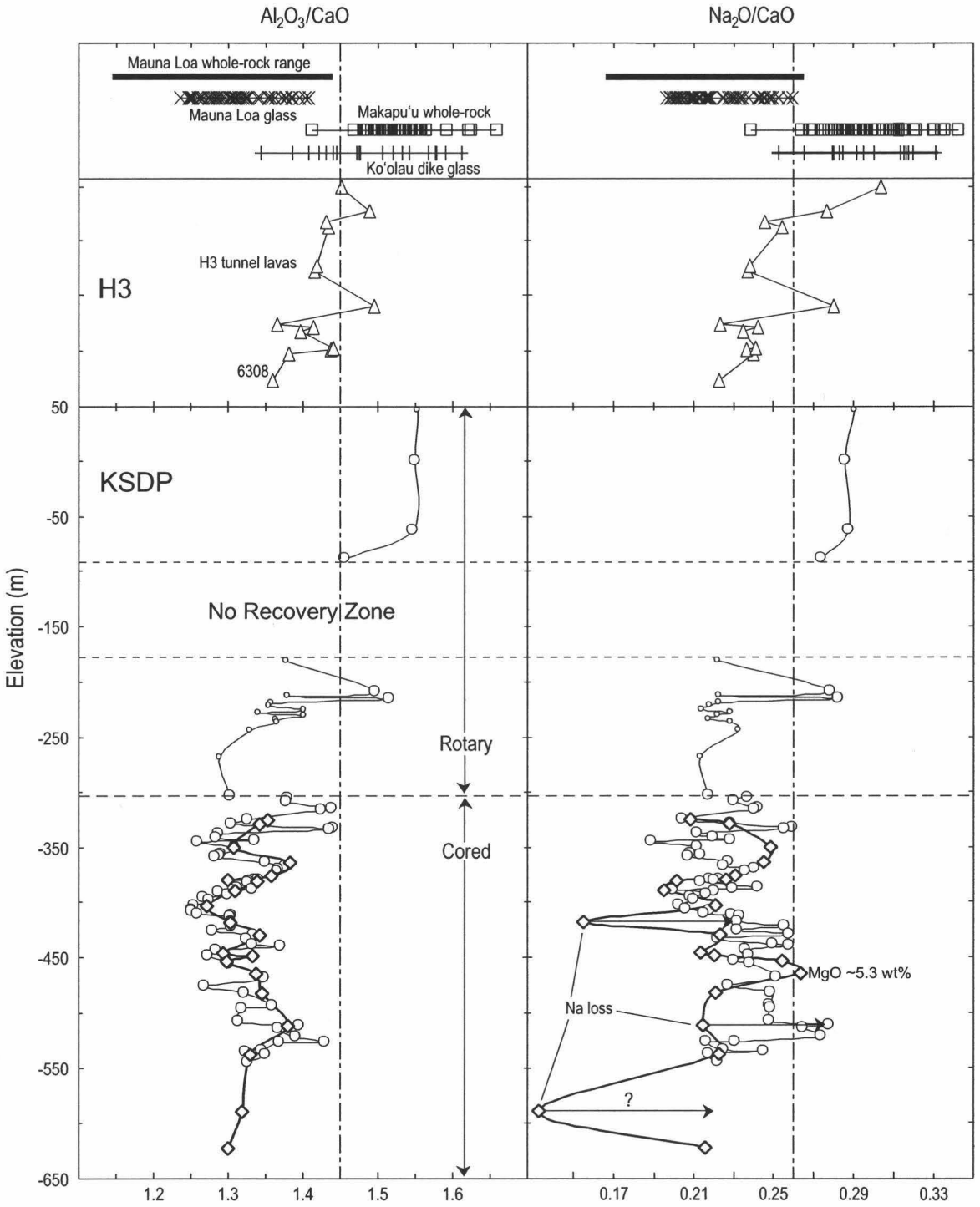

Fig. 12. Distinctive geochemical whole-rock and glass ratios for KSDP lavas vs. elevation (relative to sea level). Symbols as in previous figures or as noted. Mauna Loa whole-rock ranges from Rhodes (unpub.). All Mauna Loa lavas and glasses with <5.8 wt% MgO have been removed to reduce clinopyroxene fractionation effects. Makapu'u lavas that have experienced significant plagioclase fractionation ($Al_2O_3/CaO < 1.45$) have been removed. The relative thickness and sample locations from the H3 tunnel section are shown for comparison. Simultaneous plagioclase and clinopyroxene fractionation tends to buffer KSDP Al_2O_3/CaO. Typical subaerial Ko'olau lavas do not fractionate clinopyroxene, and moderately evolved glass compositions are dominated by plagioclase fractionation, leading to lower Al_2O_3/CaO values than whole-rock data.

Na_2O/CaO ratios typical of Ko'olau, deeper flows oscillate from KSDP to Ko'olau compositions over ~60 m. The seven deepest H3 flows sampled (from the lowest 50 m of the section) all have low Al_2O_3/CaO and Na_2O/CaO like Mauna Loa and KSDP. The entire transitional interval may be exposed at the H3 tunnels, which would then be ~60 m (42 flows) thick. Jackson et al. (1999) did not recognize that 14 of the 19 analyzed lavas from this section have both Al_2O_3/CaO and Na_2O/CaO values below those of typical Ko'olau flows, although they did emphasize the Kilauea-like geochemistry of one evolved lava from the bottom of the section.

Glass compositions from the KSDP core and subaerial Ko'olau exposures also indicate a stratigraphic change in geochemistry, although there are no glass samples from the KSDP rotary or H3 tunnel sections. The deepest glass analyses (588 and 616 mbsl) extend below the deepest unaltered whole-rock data (550 mbsl), and indicate that the Mauna Loa-like composition of Ko'olau volcano persists for at least 400 m of lava at a depth over 600 m beneath Kalihi valley. The Na_2O/CaO of unaltered samples is the best glass discriminant, as 18% of the Ko'olau glasses have low Al_2O_3/CaO values due to plagioclase fractionation. Conversely, KSDP glass samples maintain their low Al_2O_3/CaO because plagioclase fractionation is less dominant in these lavas.

Estimated Duration and Volume of Ko'olau Intrashield Stages

Estimates of subaerial Hawaiian shield-stage lava accumulation rates vary according to volcanic production rates, ages, and the location on the edifice. For example, lava accumulation rates for near-summit locations (e.g., H3 tunnels) are higher than on the flanks of Hawaiian volcanoes (e.g., KSDP site). Incomplete recovery from

the KSDP transitional interval (rotary section) makes estimates for the eruptive duration and volume of the geochemically intermediate phase from the more complete H3 tunnel section problematic, but some constraints are possible.

The 25-35 mm/year summit accumulation rate estimated for Mauna Loa (DePaolo & Stolper, 1996) can be used as a maximum value. Estimates of the coastal flanks of Mauna Loa (7.8 ±3.2 mm/yr; Sharp et al., 1996) and the east rift zone of Kilauea (up to 10 mm/yr (Quane et al., 2000), are used as a minimum. When these rates are multiplied by the ~60 m transitional interval in the H3 tunnel section, they produce a 1700-7700 year duration of geochemical fluctuation between Mauna Loa-like and typical Ko'olau geochemistry. This period represents only ~0.3-1.3% of the length of an average Hawaiian shield-building stage (550-600 ka; Guillou et al., 1997; DePaolo & Stolper, 1996), but the very existence of a transitional interval indicates a non-instantaneous change in geochemistry. Such a brief eruptive interval may produce lava flows that are only locally distributed, rather than spread evenly over the entire shield surface and therefore overestimate or underestimate actual duration and volume values. Combining our average eruptive duration with eruption rate estimates for Kilauea of 0.05 km^3/year (Quane et al., 2000; Dvorak & Dzurisin, 1993) gives an 85-300 km^3 volume of transitional material erupted.

The thickness of typical Ko'olau flows overlying the H3 transitional lavas (500-600 m; Jackson et al., 1999) indicates a much greater volume of typical Ko'olau rather than transitional lavas. As noted earlier, these uppermost flows still cover virtually the entire subaerially exposed surface of the volcano, so eruptive duration and volume estimates are based on the assumption of uniform lava flow distribution. All 35 flows

within the 200 m cored interval at the WAFB have high Al_2O_3/CaO and Na_2O/CaO values, providing further evidence of extensive eruption of typical Ko'olau tholeiites. Using the same accumulation rates mentioned above, these final shield-stage tholeiites were erupted over 14 – 77 ka or possibly longer as the end of this stage approached (Frey et al., 1991). Over this time period, 700-3000 km^3 of material could have been erupted. The lower end of this volume estimate is in agreement with a recent, independent estimate for these geochemically distinct lavas (1000 km^3; Takahashi & Nakajima, 2002).

The Effects of Differential Subsidence on Ko'olau Lava Flow Dips

The average slope of lava flows measured in the H3 tunnels (Jackson et al., 1999) and lower Kalihi is 4°. However, extension of this regional dip between sites predicts transitional geochemistry at an elevation of ~300 mbsl, near the bottom of the rotary-drilled or top of the cored section. The geochemical stratigraphy of the KSDP indicates that transitional flows are located at a maximum depth of only 182-218 mbsl, indicating a somewhat smaller regional dip (~3°).

Stratigraphic dip measurements (Table 1) show that this slight difference in regional dip is not due to thinning of the section as a result of the seaward increase in shield vs. lava flow area and the variable length of lava flows. The dip in lower Kalihi valley shows an overall decrease from 6° to 3° over 70 m of vertical exposure from the top to the base of the ridge (Table 1). A similar decrease in dip with depth at Wa'ahila ridge and Waipahu (Multhaup, 1990) supports the idea that lava flow dips decrease with depth within a Hawaiian shield (Walker, 1992). Geochemical correlations indicate that shield flow dips reverse orientation at depth and point inward toward the caldera. Such

observations are not inconsistent with modern structural models of Hawaiian shields. Moore (1987) stated that as the volcanic edifice grows, subsidence is greatest beneath the most massive central portion of the shield, which contains the greatest total thickness of lava flows and dense cumulates. Overall, lava dip deflection caused by subsidence of the shield may be proportional to summit proximity and age of the flow.

Field observations and the above arguments lead us to believe that the flows sampled by the KSDP at a depth of ~180 mbsl traveled ~7.5 km from their eruptive source over a regional dip that has subsided and now averages only ~3°. The 4° dip of lava flows measured at the H3 tunnels is an average dip, irrespective of depth within the shield, which is within the error of measurement for approximating the regional dip. Differential subsidence of the Ko'olau shield has reduced the angle of its relatively uneroded slopes (planezes), but has not caused significant regional lava flow dip variability among the subaerially erupted flows sampled in this study. A comparison of representative profiles across parts of the unbuttressed flanks of Ko'olau and Mauna Loa (Walker, 1990) reveals consistently lower slopes for Ko'olau, indicating that subsidence and erosion of Mauna Loa may eventually produce planezes of similar slope.

Modeling the Component of Recycled Oceanic Crust in the Hawaiian Source

The hypothesis that the Hawaiian source contains a component of recycled oceanic crust (Hofmann, 1982), has become widely accepted. Studies of incompatible trace element and isotopic signatures (Lassiter & Hauri, 1998; Sobolev et al., 2000) have shown that variable degrees of melting of the peridotitic mantle alone cannot produce the compositions of some Hawaiian lavas. High incompatible trace element abundances,

high Sr anomalies in melt inclusions contained in olivine, and Os isotopic data from individual volcanoes indicate that subducted oceanic crust is metamorphosed to eclogite and melted to form a significant source component for some Hawaiian magmas (e.g. Hauri, 1996). Melting experiments involving peridotite and basalt (Yaxley & Green, 1998; Takahashi & Nakajima, 2002) of appropriate composition would therefore be expected to produce the parental melts of Hawaiian volcanoes under the right pressure and temperature conditions.

Using the thermodynamically-based and experimentally calibrated MELTS program (Ghiorso and Sack, 1995), the evolution of selected parental liquids created from high-pressure (2.7-3.0 GPa) melting experiments (Takahashi & Nakajima, 2001) was modeled. These experiments used Archean basalt (thought to more closely resemble the composition of ancient subducted oceanic lithosphere than modern MORB), and sandwiches of mantle peridotite with Archean basalt. Our goal in modeling was to evaluate whether the resulting liquids, if unmodified during ascent, evolve along paths defined by KSDP, Ko'olau, or Mauna Loa glass data. For comparison, we also modeled the evolution of typical Mauna Loa olivine-hosted melt inclusions determined from 160 analyses from three picrite flows (supplementary information from Sobolev et al., 2000), and typical Ko'olau melt inclusions determined from 111 analyses of two picritic basalts (Norman et al., 2002). Pressure and oxygen fugacity values selected are from Davis et al. (2000), and initial water content is based olivine-hosted melt inclusion values from Hauri (2002). Model conditions are listed in Table 9.

None of the experimental melts could be modeled to match KSDP and Mauna Loa or Ko'olau compositions (Fig. 13). For example, model Al_2O_3 crystal fractionation

paths are too high to match any Hawaiian tholeiite. In addition, the high MgO (16.8 wt%; Sobolev et al., 2000) of Mauna Loa inclusions was only attained in sandwich melting experiments where the melt fraction reached 85%, an unrealistically high value. In contrast, the average melt inclusion compositions from Mauna Loa and Ko'olau are more reasonable parent compositions. If melt inclusion compositions are better parent magmas, then successful melting experiments should at least reproduce the inclusion compositions. However, none of the experimental melts are consistently within the range of Ko'olau melt inclusion compositions. If Archean basalt is a component of typical Ko'olau as well as KSDP and Mauna Loa parental melts, then the correct composition, temperature, and pressure under which these melts are created has not yet been found.

Processes Influencing the Ko'olau Source

Incompatible trace elements are more sensitive than major elements to source composition and degree of melting, and KSDP lavas have incompatible trace element abundances intermediate between those of Mauna Loa and Ko'olau. The fact that all Ko'olau incompatible element abundances are greater at a given MgO than those of Mauna Loa (Fig. 10) is most likely the result of a lower degree of melting in the Ko'olau source (Norman & Garcia, 1999). However, the assumption that Ko'olau lavas are the product of a similarly low degree of melting as Loihi tholeiites (Norman & Garcia, 1999) is no longer valid in light of the geochemical and petrographic similarities observed between Ko'olau, KSDP, and Mauna Loa lavas in this study. However, Norman & Garcia have demonstrated that surface Ko'olau lavas can be created by the addition of recycled oceanic crust to a Mauna Loa-like (KSDP) source. While lower degrees of

Table 9. MELTS parental magma information. Melts were created under the conditions listed (Takahashi & Nakajima, 2002).

Parental material (Fig. 12 abbreviation)	MgO (wt%)	P (GPa)	T (°C)	F
Archean basalt melt (AB)	7.6	2.7	1425	0.85
Fertile peridotite and archean basalt sandwich melt (ABP1)	7.8	3.0	1475	0.4
Fertile peridotite and archean basalt sandwich melt (ABP2)	12.5	3.0	1500	0.8
*Average Mauna Loa olivine inclusion (OIML)	16.9	-	-	-
†Average Ko'olau olivine inclusion (OIKO)	11.7	-	-	-

*From Sobolev et al., 2000; average of 160 analyses from three picrites.
†From Norman et al., 2002; average of 111 analyses from two picrites.
F = melt fraction

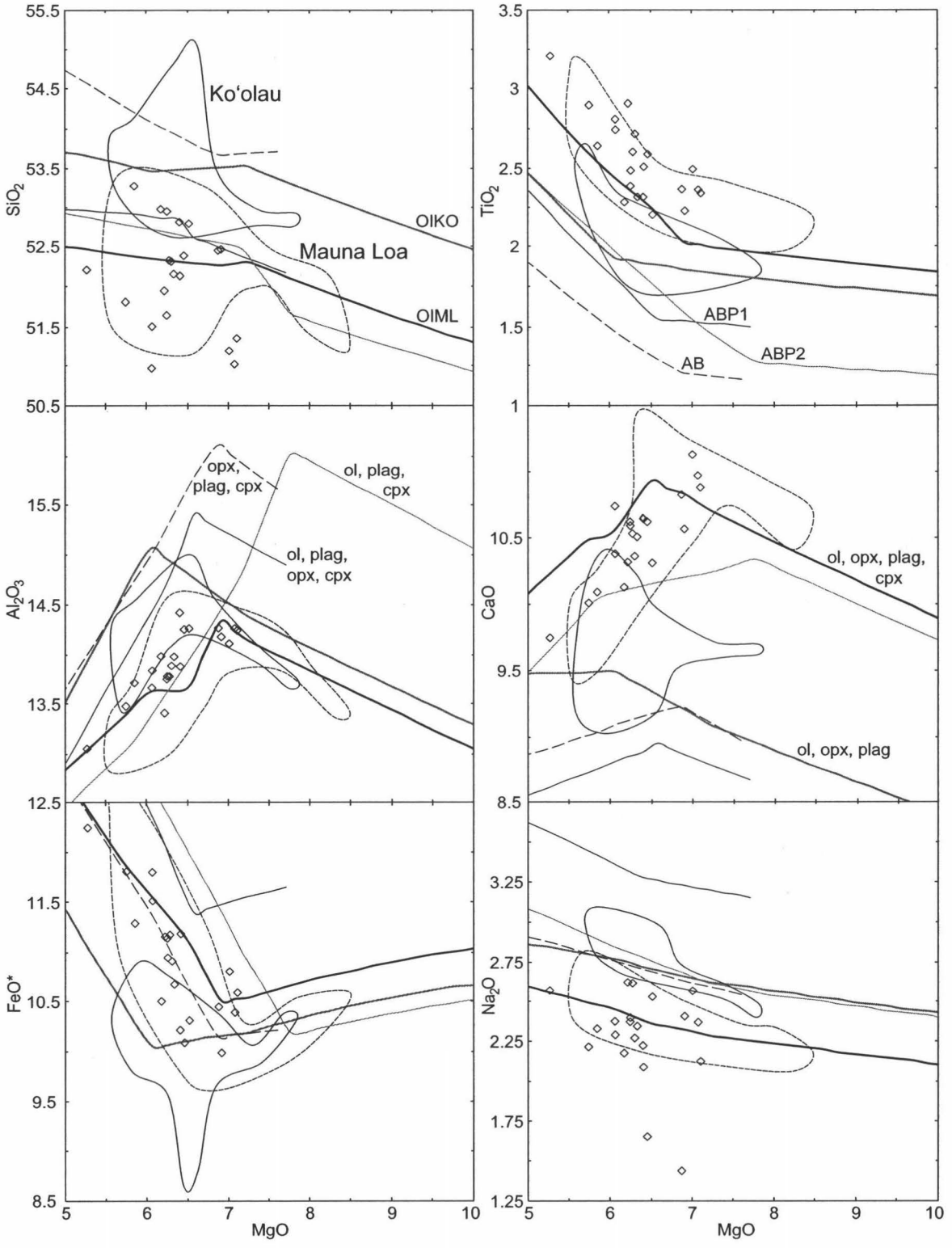

Fig. 13. Fractional crystallization paths of experimentally created potential Hawaiian magma parents (Takahashi & Nakajima, 2002) as well as representative Ko'olau and Mauna Loa olivine inclusions (Norman et al., 2002; Sobolev et al., 2000) compared to KSDP, typical Ko'olau, and Mauna Loa glass compositions. Paths determined using MELTS (Ghioso & Sack, 1995). Path labels indicate starting material(s) as shown in Table 8 and crystallization sequences. All melts were crystallized at 0.5 kbar, QFM-1, and 0.1 wt% H_2O. See text for discussion.

melting can explain the higher Na_2O, Al_2O_3, and lower CaO abundances of surface Ko'olau flows, Norman & Garcia (1999) have shown that the high Sr/Y values of surface Ko'olau lavas cannot be created without melting another component, while the low Sm/Nd of Ko'olau is from high Nd abundances – a signature commonly inherited from recycled oceanic crust and/or sediments.

Either the addition of melt from recycled oceanic crust or a reduction in the dominance of mantle-derived melts could drive the geochemical transition from KSDP to surface Ko'olau lavas. The overwhelming evidence for recycled material in the Hawaiian source leads us to believe that the latter interpretation is more correct. As the degree of source melting decreases due to movement of the volcano past the hot spot, recycled oceanic crust should constitute a larger component of the melt because its melting point is lower than that of mantle peridotite. This explanation produces the higher abundances of incompatible elements and SiO_2, as well as trace element and isotopic signatures.

Rare high-Sr melt inclusions in Mauna Loa olivines (Sobolev et al., 2000) and the high Sr abundances of Ko'olau lavas examined in this study suggest a Sr-rich source for both of these volcanoes. The gabbroic component of recycled oceanic crust contains plagioclase cumulates, which are the most likely source of this Sr enrichment (Sobolev et al., 2000). This component was not included in the melting experiments of Takahashi & Nakajima (2002). In addition, the presence of ~3% subducted pelagic sediments is required to reproduce Ko'olau Os and Pb isotopic signatures (Bennett et al., 1996), and these sediments were absent from melting experiments as well. Archean basalt is only a single component of the material that is subducted, metamorphosed to eclogite, and later

melted and mixed with mantle melts to form the parental magmas of Ko'olau volcano.

A catastrophic unloading event such as the Nu'uanu landslide could not have caused the change in Ko'olau shield-stage geochemistry, because a decrease in the overlying pressure would be expected to produce a higher degree of melting. Only if volcanic activity stopped completely after KSDP-type lavas were erupted and was later revived by unloading could the Nu'uanu landslide have played a role in creating surface Ko'olau lavas. However, there is no geologic evidence of post-landslide shield-stage eruptions anywhere on the volcano, so we reject this hypothesis.

CONCLUSIONS

The ~2.9 Ma KSDP lavas display a rapid change in geochemistry within Ko'olau volcano from Mauna Loa to Makapu'u-like flows, which occurs at an elevation of 182-215 mbsl beneath lower Kalihi Valley. This change occurs within the rotary-drilled section of the hole, ~100 m shallower than predicted from field measurements. However, considering the locally variable nature of tholeiitic lava flow emplacement and the subsequent difficulties of correlating flow units on Hawaiian shields, our 1° overestimate of the regional flow dip over a 7.6 km section of the SW flank of Ko'olau volcano is remarkably accurate. The geochemical transition occurred relatively abruptly (over only 2000 – 7700 years) when compared to the periods of geochemically distinct shield building that preceded and succeeded it. However, the existence of a transitional interval indicates that the process that caused it was more gradual than a catastrophic unloading event such as the Nu'uanu landslide might produce. Such a rapid and large-scale change in shield-stage major element geochemistry is unique among Hawaiian volcanoes, but

could simply be the result of a decrease in the overall extent of source melting due to movement of the volcano off the hot spot and a larger role for recycled oceanic crustal melts. Small differences in both degree of melting (F) and source composition can produce the observed major and trace element compositions of Mauna Loa, KSDP, and Ko'olau lavas. Recent attempts at experimentally creating the parental melts of Hawaiian tholeiites (Yaxley & Green, 1998; Takahashi & Nakajima, 2002) have been less successful than studies of olivine-hosted melt inclusions, which appear to contain remnants of these parental melts whose crystallization paths can be modeled to match their respective volcano's glass compositions.

APPENDIX

The KSDP Web Site

The Drilling Information System (DIS) database and the KSDP web site were used to organize the vast amount of information collected at the drill site and to present it to the community of KSDP researchers who are following the progress of the project from around the globe. The international nature of the KSDP makes the internet an especially valuable tool for exchanging information and consolidating research efforts.

Throughout the duration of drilling and logging in Kalihi, information was entered into the DIS database and uploaded daily to the HSDP web site to allow cooperating researchers to have near real time access to project data. Data packages contained updates on all information collected at the site for that day, including core run and box depths, core logs, digital photographs of core boxes and drill site activity, and reports on drilling activities and progress. Archives of the daily data reports are available on the KSDP web site along with the summarizing tables and core logs. In addition, images of the core boxes can be viewed on the web. GeoForschungsZentrum Potsdam (GFZ) in Germany currently maintains the site, located at http://icdp.gfz-potsdam.de/html/koolau/news.html.

The Drilling Information System (DIS) Database and the DIS web interface

The DIS database is a customized Microsoft Access database developed by Ronald Conze (Operational Support Group ICDP at GFZ) and Frank Krysiak (Smartcube Ltd., Germany). The general structure of the database is organized to record all

information collected during a drilling project. Specific data structures and input forms were tailored to the needs of HSDP and were modified as needed during the course of that project. Within the database are standardized input forms for core logging, sample information, and other drilling data. Eric Haskins and Michael Garcia performed core logging and data entries into DIS during the KSDP. The use of standardized logging and data input forms helped to ensure that core loggers evaluated a consistent set of criteria and that data were entered in the database in the proper format and style. For more information about the DIS or the HSDP web site, contact Ronald Conze (conze@gfz-potsdam.de).

Core Handling Procedures – after those developed by the HSDP

A prerequisite for the success of the KSDP is the acquisition and documentation of continuous cores in stratigraphic sequence. The procedures for core handling and preparation, the splitting of the core into working and archive halves, and primary core descriptions are described here.

Wire-line core drilling was conducted weekdays eight hours a day, except on holidays. Handling and curation procedures began when the inner core barrel was removed from the hole. After consultation with the core driller, the drilling hands under the supervision of the core driller removed core from the inner core barrel. In order to minimize contamination of the core, no smoking was allowed nearby (phosphorous and rare earth elements) and all hand jewelry was removed (platinum group elements).

1. Removal of the core from the core barrel

    a) The core was removed from the core barrel by the drilling crew and placed in sequentially numbered 6' PVC trays. A core logger was usually present to observe and assist if needed. The PVC trays were securely mounted on 8" wide planks, which provided stability and allowed drainage of water and drilling mud through ~5 mm diameter holes spaced evenly along the tray bottoms when they were rinsed. Orange paint was used to mark the tops of the trays, and drillers were careful to place the top of the core at the top of the tray. Once the trays were filled with core, they were fitted with end blocks and PVC top covers. The core trays were carried to the processing area by the core logging team.

    b) For each core run, the drilling crew or a core logger prepared a wooden block with the core run number, the top and bottom driller's depths, and the amount of core recovered. The wooden block was placed at the top of the appropriate PVC core tray. Each core run was completely washed, marked, and boxed. For each core run, the core processing team checked that the PVC trays were properly oriented and arranged in sequence and that the information on the wooden block was correct.

2. Washing

    a) The core trays were laid out on the core-washing area with the trays for each run arranged in sequence.

b) The core was washed carefully and thoroughly using water hoses and brushes to remove drilling mud and rock cuttings. Special care was taken during the washing of soil or non-coherent core to prevent disruption or loss of core.

c) After washing, the core loggers reviewed the core. Any unusual geologic features and contacts were identified and noted. This core review also helped to identify any mix-ups or misorientations of the core that occurred during handling.

3. Run information and core boxing

a) Individual core runs were placed on working tables for preliminary logging. A Run Information Form (RIF; see example forms at end of Appendix) was filled out for each core run. The run number, driller's depths, date, and any unusual conditions related to the recovery of the core were noted on the RIF.

b) The core was aligned, and individual pieces were fitted together where possible. The top of the core run being processed was compared to the bottom of the previous core run, and it was noted on the RIF whether these two pieces of core could be fitted together. The length of recovered core was measured in feet (to the nearest tenth) and this was recorded on the RIF. This length included the best estimates for lengths of rubble zones. Sometimes, measured core recovery recorded on the RIF exceeded recovery reported by drillers. This may be caused by the difficulty of estimating the length of these rubble sections, or core left over from a previous run and picked up by the next run.

c) The core was then marked for "up" orientation with blue and red, permanent, waterproof felt-tipped pens. If necessary, the surface of the core was first dried

with a heat gun to prevent smudging of the pen marks. Orientation lines were marked twice on the core, on opposite sides, so that when the core was split into working and archive portions, each piece retained a set of lines.

d) Black lines were drawn circumscribing the core at 1-ft intervals starting at the top of each run. The intervals were marked with the run number and depth, in feet, below the start of the run. Depth intervals within rubbly sections were estimated, and Styrofoam blocks labeled with the run number and depth were placed in the rubble zones at 1-ft intervals.

e) Delicate (e.g., ash or soil) or highly fractured or rubbly core (common in a'ā clinker zones) was bound in shrink-wrap to preserve its integrity.

f) Preliminary identification of units was made and the location of contacts and unusual features (e.g., delicate glass-bearing sections, secondary mineralization, ash layers or baked contacts) were noted on the RIF. Any special instructions for slabbing were added to the form as well.

g) The core was put into plastic core boxes that were segmented into five 2-ft long rows. The boxes were marked with top and bottom labels and oriented with the top of the box at the upper left corner. Core was placed in the box beginning with the top in the upper left corner, and continuing down and to the right (see example figures at end of Appendix).

h) If necessary, the core was cut with a saw so that each 2-ft segment fit in the core box exactly. A Styrofoam block was placed at the end of each run, labeled with the core run number and the ending driller's depth for that run and the core run number and driller's starting depth for the next run. Additional unlabeled

Styrofoam blocks were placed in boxes to minimize movement of the core during transport.

i) After each plastic core box was filled, it was labeled with a black waterproof felt-tipped pen. The project name (KSDP), the box number, the core run number (or run numbers if the box contains material from more than one core run) and the driller's depth range of the core segment in the box were all noted on the box and its lid. The box numbers in which each run was stored were recorded on the RIF.

4. Core slabbing

The core was cut lengthwise between the two sets of orientation lines to create "archive" and "working" splits of the core. The saw was set up so that the archive split was about one third of the core and the working split the other two thirds. If the core contained special features, an attempt was made to preserve them in both splits of the core. Core was lightly rinsed after slabbing and placed into the core boxes.

5. KSDP Core boxes

a) After slabbing, the core was returned to its original plastic core box. The open core box was put out in the sun until the newly slabbed surface was dry enough to mark. After drying, foot markers, run numbers

and depths, and arrows pointing to the top of the core were marked on the cut faces of the core with a blue waterproof felt-tipped pen. Any markings on the back of the core that had become obscured or removed during slabbing were remarked.

b) Once marked, the open face of the working split in the core box was digitally photographed. A Kodak Color Separation Guide (No. Q-14) and scale were

placed adjacent to the core box, along with the box number clearly written on an index card. This digital image was adjusted (rotated, cropped, color corrected and lightened etc.), and given the box number as a file name. An entry was then made into the DIS database for each working box photo, which could later be pulled up and annotated by the logger.

c) The core in each core box was then ready for logging. Logging procedures are described in detail in the following section. After logging, each core box was covered with its lid and stacked at the logging area to await later on-site sampling. Only the working portion of the core was sampled.

Core Logging Procedures

Logging (the hand-specimen scale description of the core) is critical to the success of the KSDP since it provides the framework for all subsequent sampling and scientific study of the core. Logging was done only on the working split of the core. To ensure the quality and consistency of the core logging, several steps were taken. First, all data was entered directly into the DIS database, using standardized logging forms. Second, the chief logger, Mike Garcia, reviewed and edited the work of logger Eric Haskins to ensure accuracy.

Standardized logging forms for lava flows, tephra, and sedimentary units were based on protocols from Ocean Drilling Program (Shipboard Scientists Handbook, Ocean Drilling Program, Texas A&M University, ODP Tech, Note No. 3, 1990), the Creede Caldera Moat Scientific Drilling Project (USGS Open File Report 92-410), the State of Hawaii - Scientific Observation Hole coring project (USGS Open File Report 92-586),

the HSDP pilot hole (Stolper et al. 1994, Core Logs) and Long Valley Drilling Project (USGS Open File Report 99-158).

Loggers used a hand lens, ruler (metric and inches in tenths), references on rock and mineral classification, a clear plastic 100-point grid for point counting, dilute hydrochloric acid, a hardness test kit, and a protractor. The log for each box of core consists of two parts: an annotated digital photograph of the box and a written description of the core prepared using the standardized logging forms.

1. Identifying contacts and defining box units

The core in each working box was divided into box units (lettered from a to z, from the top of each box) based on the presence of contacts (e.g., the occurrence of glassy margins, baked contacts, and/or changes in lithology). Top and bottom depths of the box and the top depth for each unit in the box were recorded relative to the top depth of each run. All absolute depths were automatically calculated in the database from the relative depth information entered by the logger.

a) The type of top and bottom contact was identified, and the logger made a brief description of the criteria used in identifying the contact. Choices of contact type available in pull-down menus on the logging form were: **continuous with next/previous box, depositional, flow contact, flow over sediment,** or **missing** (logging descriptions made by choosing from pull-down menus on the logging form are listed in bold type, and definitions of the descriptions are shown in parentheses following the menu item).

b) For lavas, the groundmass texture was determined (**glassy, cryptocrystalline, microcrystalline, fine grained** (<1 mm), **medium grained** (1-2 mm), **coarse grained** (>2 mm)). Comments on the groundmass (e.g., mineralogy and texture) were added when relevant.

c) Vesicle abundance was noted from the point count or visually estimated in volume % (**sparse** (<5%), **moderate** (5-15%), **abundant** (15-30%), **very abundant** (>30%), and **variable**). Average vesicle size (small <1 mm, medium 1-5 mm, and large >5 mm), shape (round, sub-rounded, sub-angular, angular), and aspect ratio (equant, horizontally elongated, vertically elongated, inclined - if inclined, the dip relative to the axis of the core was included) were recorded. Comments were also made on the vesicle distribution within the unit.

d) The extent of alteration was estimated in volume % of the core as a whole (excluding alteration along fractures): **fresh** (<2% alteration), **slightly altered** (2-10% alteration), **moderately altered** (10-40% alteration), **highly altered** (>40% alteration). Where fresh glass and unaltered olivines were present but secondary minerals also occurred, the rock was classified as **slightly altered**. Secondary minerals were described (hardness, color, luster, crystal habit, etc.) and identified where possible (e.g., clays, zeolites, etc.). Comments on the mode of occurrence of the alteration minerals in the unit, (e.g., vein or fracture fillings, etc.) were made.

e) The extent of fracturing was estimated based on the number of fractures/foot (**none, weakly fractured**, (<4 fractures/ft), **moderately fractured** (4-10 fractures/ft), **highly fractured** (>10 fractures/ft), or **rubble**).

f) When appropriate, sedimentary features were described (e.g., grain size, sorting, and dip of bedding).

g) Any additional comments on the unit were added as appropriate. Features of interest were noted on the box photograph.

2. Point counts

A point count was made for each lithologic flow unit (except those units that were so altered that their phases were unrecognizable). The total abundance of all phenocrysts and vesicles >1 mm in the rock was determined based on a 100-point count on a representative portion of the core. Point counts were done with a 10x hand lens using a transparent sheet printed with 100 grid intersections. If a mineral was observed in a box unit, but was not abundant enough to appear in a point count, its abundance was recorded as 0.1%. If there was substantial variation in mineralogy within a unit, additional point counts were made. Point count locations were marked on the box photograph with a rectangle and labeled "pc." Classification of the volcanic rocks used the following ranges: **aphyric** (<1%), **sparsely phyric** (1-2%), **moderately phyric** (3-10%), **highly phyric** (>10%). Comments on the overall phenocryst population, such as distribution (**even** or **uneven**), size (**small** (<1 mm), **medium** (1-5 mm) or **large** (>5 mm)), and crystal shape (equant, tabular, euhedral, subhedral, or anhedral) were added to each point count description. Some point counts were done on the back of the core, in which case this was noted in the comments to the point count. However, the point count location was marked on the face of the core at the appropriate place on the digital image of the core box.

3. Internal boundaries

When internal boundaries were present within units (e.g., lobes of a pāhoehoe flow marked by glassy and/or ropy surfaces), their depths were recorded and their locations were marked with thin dashed lines on the digital image of the core box.

4. Lithologic Units

Once a group of boxes had been logged, the logger and chief logger reviewed the logs and assigned rock names to lithologic units. Rock names were based on the abundance and identity of phenocryst phases, as well as vesicularity. For example, a basalt with > 25% vesicles, a 3-10% total phenocryst content with both olivine and plagioclase phenocrysts (but olivine>plagioclase) was called a "highly vesicular, moderately plagioclase-olivine-phyric basalt," following the style described by the IUGS Subcommission on the Systematics of Igneous Rocks (1989) with the addition of vesicularity information. If the variation in phenocryst abundance in a unit spanned the limits of pre-defined ranges, it was given a name that reflected the variation in abundance. For example, a unit with olivine content ranging from 7 to 13% would be called "moderately-to-highly olivine-phyric basalt." In addition to assigning rock names, the chief logger proofread and edited all other logs to minimize inconsistencies and ambiguities.

Sampling

Petrographic and geochemical characterization of the KSDP sequence of lavas is one of the primary goals of this project. A suite of reference samples was collected on-site for the preparation of polished thin sections and powders to be distributed for

geochemical analyses. Reference samples for geochemical analysis were taken from the interior of the core, and altered fractures of areas with vesicle fillings were avoided. Flow and intraflow glass was also sampled from the core for electron microprobe analysis.

The whole-rock sample size was typically about 800 g. A thin section blank was cut from the same area as each powder sample. Samples were labeled by the run and relative depth of their tops as a unique identifier (e.g., R103-12.9) and recorded in the DIS database. Styrofoam blocks labeled in red with flow unit numbers were inserted into the spaces left by core removal. Thin section blanks were cut from the core after the reference samples were collected. The reference suite was sent to UMass, where each rock sample was coarsely crushed. Following coarse crushing, approximately one half of the powder was reserved for investigators who require mineral separates. The remaining powder was finely crushed, and powders were distributed to investigators according to their proposed analytical procedure. Unsampled core is currently stored at the UH Marine Center in Honolulu.

KOOLAU SCIENTIFIC DRILLING PROJECT
Run Information Sheet

Date 11-5-00 (Day-Month-Year) **Run Logger** MG (EH) ___

Run Number 82

Top Depth (from drillers) 1840 **Ft.** **Bottom Depth** 1850 **Ft.**

Recovery (total amount actually recovered) 10.2 **Ft.**

Continuous with previous core? Yes (No)

Top Box Number 71 **Bottom Box Number** 72

Flow Type pahoehoe

Contact baked interflow at 7.5-8'

Mineralogy divine and plagioclase

Vesicularity high to moderate throughout most of run

Alteration weak to moderate → some secondary minerals in voids + fractures

Remarks/Special Features: Vesicularity increases significantly below 7.5-8' contact

box unit #:	B0021b	unit #:	U0023
core box #:	B0021	box unit:	b
logged by:	EH		
core run	R0029	distance to top of run:	0.7
calculated top depth:	1354.7		
rock name:	Variably vesicular, aphyric basalt		
top contact:	flow contact		
bottom contact:	flow contact		
contact comments:	The top contact is made up of three pieces of core located in the middle of the second row of the box. The bottom contact is mostly missing, but visible in the uppermost piece of core in the fifth row.		
groundmass:	cryptocrystalline		
groundmass / matrix comments:			
vesicularity:	variable		
vesicles comments:	This unit is moderately to highly vesicular and contains autoliths (see core at top of fourth row of box).		
alteration:	moderate		
alteration comments:	The only fresh piece of core in this unit is located at the top of the fourth row (R31-0.6).		
fractures:	highly		
fractures comments:	Most of this unit is rubble, although there are a few pieces of well-consolidated core.		
sedimentary comments:			
general comments:	There is a glassy, high-angle intraflow contact present at R31-1.5. This box unit = litho unit #23.		

box unit #: B0021b

point count ID: 36

core run #: R0031

distance from top of run: 1.4

calculated top depth: 135974

Components		size	distribution
olivine %:	0 000		
comments:			
plagioclase %:	0 000		
comments:			
clinopyroxene %:	0 000		
comments:			
vesicles %:	17	medium	uneven
comments:	Vesicles become smaller and more abundant toward the intraflow contact. The smallest vesicles are <1 mm.		
groundmass %:	83 000		
comments:			
general comments:	Point count taken on the upper part of the core piece that contains the high-angle intraflow contact.		

unit #:	U0023	sub unit:	
core run #:	R0029		
top box unit #:	B0021b	underlying box unit #:	B0021c
top depth:	13547	bottom depth:	13603
top contact:	flow contact		
bottom contact:	flow contact		
unit class:	VOL		
unit type: transitional	pahoehoe		
rock name:	~~Moderately altered~~, variably vesicular, aphyric basalt		

icdp

Rock Coring Koolau Volcano

Core Logging Summary Report

soest university of hawai'i

Run on Top of Box	Distance to Top Run	Top Depth of Box	Interval	Box #:
R0028	0.3	1346.3		
Run on Bottom of Box	**Distance to Bottom Run**	**Bottom Depth of Box**	15.7	B0021
R0031	4	1362		

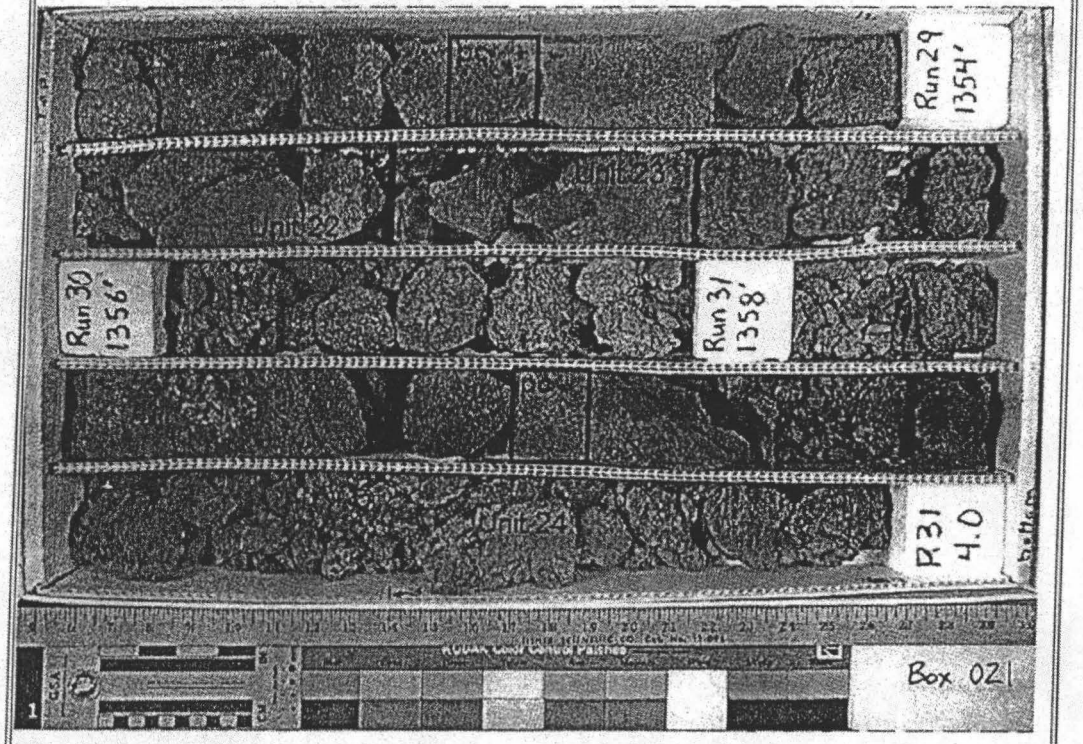

Core Run - Distance:
R0029 - 0.7
Calculated Top Depth:
1354.7
Unit Class - Unit Type:
VOL - transitional
Rock Name:
Variably vesicular, aphyric basalt.
Top Contact:
flow contact
Bottom Contact:
flow contact
Logged By:
EH

BOX UNIT:
B0021b

B0021b (1354.7 feet)
Show Report

UNIT:
U0023

Contact Comments	The top contact is made up of three pieces of core located in the middle of the second row of the box. The bottom contact is mostly missing, but visible in the uppermost piece of core in the fifth row.
Groundmass/Matrix	cryptocrystalline
-	
Vesicles Abundance	variable
-	This unit is moderately to highly vesicular and contains autoliths (see core at top of fourth row of box).
Alteration	moderate
-	The only fresh piece of core in this unit is located at the top of the fourth row (R31-0.6).
Fractures	highly
-	Most of this unit is rubble, although there are a few pieces of well-consolidated core.
Sediment Comments	
General Comments	There is a glassy, high-angle intraflow contact present at R31-1.5. This box unit = litho unit #23.

POINTCOUNT AREA

Run: R0031

Distance to Top of Run: 1.4

Calculated Top Depth: 1359.4

Component:	%	norm.	Size:	Distribution:	Comments:
Olivine:	0	0.00			
Plagioclase:	0	0.00			
Clinopyroxene:	0	0.00			
Vesicles:	17		medium	uneven	Vesicles become smaller and more abundant toward the intraflow contact. The smallest vesicles are <1 mm.
Groundmass:	83	1.00			

General Comments: Point count taken on the upper part of the core piece that contains the high-angle intraflow contact.

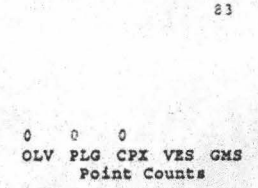

REFERENCES

Bennett, V. C., Esat, T. M., Norman, M. D. Two mantle-plume components in Hawaiian picrites inferred from correlated Os-Pb isotopes. Nature (London), 381 (6579), p. 221-224. 1996.

Budahn, J. R., Schmitt, R. A. Petrogenetic modeling of Hawaiian tholeiitic basalts; a geochemical approach. Geochimica et Cosmochimica Acta, 49 (1), p. 67-87. 1985.

Campbell, Wayne R. Sampling handling and curation protocol for the Creede Caldera Moat scientific drilling project. Open-File Report - U. S. Geological Survey, OF 92-0410. 1992.

Cande, S. C., Kent, D. V. Revised calibration of the geomagnetic polarity timescale for the Late Cretaceous and Cenozoic. Journal of Geophysical Research, B, Solid Earth and Planets, 100 (4), p. 6093-6095. 1995.

Carey R. Paleomagnetism and magnetostratigraphy of the Koolau scientific drilling project core, Oahu, Hawaii. DOSECC Summer Internship Report. 2001.

Chappell, B. W. Trace element analysis of rocks by X-ray spectrometry. Barrett, C. S., Gilfrich, J. V., Noyan, I. C., Huang, T. C., Predecki, P. K. (eds). Proceedings of the Thirty-ninth annual conference on Applications of X-ray analysis. Advances in X-Ray Analysis, 34, p. 263-276. 1991.

Clague, D. A., Dalrymple, G. B. The Hawaiian-Emperor volcanic chain; Part I, Geologic evolution. Decker, R. W., Wright, T. L., Stauffer, P. H. (eds). Volcanism in Hawaii, U. S. Geological Survey Professional Paper, Chapter 1. P 1350, p. 5-73. 1987.

Clague, D. A., Frey, F. A. Petrology and trace element geochemistry of the Honolulu Volcanics, Oahu; implications for the oceanic mantle below Hawaii. Journal of Petrology, 23 (3), p. 447-504. 1982.

Compton, R.R. Manual of Field Geology, Wiley and Sons, New York. 1962.

DePaolo, D. J., Stolper, E. M. Models of Hawaiian volcano growth and plume structure; implications of results from the Hawaii Scientific Drilling Project. Journal of Geophysical Research, B, Solid Earth and Planets, 101 (5), p. 11,643-11,654. 1996.

Davis, M. G., Garcia, M.O., Wallace, P. Volatiles in Mauna Loa glasses: Implications for crustal structure. Eos 81, WP256. 2000.

Doell, R. R., Dalrymple, G. B. Potassium-Argon ages and paleomagnetism of the Waianae and Koolau Volcanic Series, Oahu, Hawaii. Geological Society of America Bulletin, 84 (4), p. 1217-1241. 1973.

Dvorak, J. J., Dzurisin, D. Variations in magma supply rate at Kilauea Volcano, Hawaii. Journal of Geophysical Research, B, Solid Earth and Planets, 98 (12), p. 22,255-22,268. 1993.

Eiler, J. M., Farley, K. A., Valley, J. W., Hofmann, A. W., Stolper, E. M. Oxygen isotope constraints on the sources of Hawaiian volcanism. Earth and Planetary Science Letters, 144 (3-4), p. 453-468. 1996.

Feigenson, M. D., Hofmann, A. W., Spera, F. J. Case studies on the origin of basalt; II, The transition from tholeiitic to alkalic volcanism on Kohala Volcano, Hawaii. Contributions to Mineralogy and Petrology, 84 (4), p. 390-405. 1983.

Frey, F. A., Garcia, M. O., Roden, M. F. Geochemical characteristics of Koolau Volcano; implications of intershield geochemical differences among Hawaiian volcanoes. Geochimica et Cosmochimica Acta, 58 (5), p. 1441-1462. 1994.

Frey, F. A., Garcia, M. O., Wise, W. S., Kennedy, A., Gurriet, P., Albarede, F. The evolution of Mauna Kea Volcano, Hawaii; petrogenesis of tholeiitic and alkalic basalts. Journal of Geophysical Research, B, Solid Earth and Planets, 96 (9), p. 14,347-14,375. 1991.

Furnes, H. Experimental palagonization of basaltic glasses of varied composition. Contributions to Mineralogy and Petrology, 50 (2), p. 105-113. 1975.

Garcia, M. O. Petrography and olivine and glass chemistry of lavas from the Hawaii Scientific Drilling Project. Journal of Geophysical Research, B, Solid Earth and Planets, 101 (5), p. 11,701-11,713. 1996.

Garcia, M. O., Muenow, D. W., Aggrey, K. E., O'Neil, J. R. Major element, volatile, and stable isotope geochemistry of Hawaiian submarine tholeiitic glasses. Journal of Geophysical Research, B, Solid Earth and Planets, 94 (8), p. 10,525-10,538. 1989.

Ghiorso, M. S., Sack, R. O. Chemical mass transfer in magmatic processes; IV, A revised and internally consistent thermodynamic model for the interpolation and extrapolation of liquid-solid equilibria in magmatic systems at elevated temperatures and pressures. Contributions to Mineralogy and Petrology, 119 (2-3), p. 197-212. 1995.

Gramlich, J. W., Lewis, V. A., Naughton, J. J. Potassium-argon dating of Holocene basalts of the Honolulu volcanic series. Geological Society of America Bulletin, 82 (5), p. 1399-1404. 1971.

Guillou, H., Turpin, L., Garnier, F., Charbit, S., Thomas, D. M. Unspiked K-Ar dating of Pleistocene tholeiitic basalts from the deep core SOH-4, Kilauea, Hawaii. Chemical Geology, 140 (1-2), p. 81-88. 1997.

Haggerty, S., Baker, I. The alteration of olivine in basaltic and associated lavas; part I, High temperature alteration. Contributions to Mineralogy and Petrology, 16 (3), p. 233-257. 1967.

Hauri, E. H. SIMS analysis of volatiles in silicate glasses, 2: isotopes and abundances in Hawaiian melt inclusions. Chemical Geology, 183, p. 115-141. 2002.

Hauri, E. H., Lassiter, J. C., DePaolo, D. J. Osmium isotope systematics of drilled lavas from Mauna Loa, Hawaii. Journal of Geophysical Research, B, Solid Earth and Planets, 101 (5), p. 11,793-11,806. 1996.

Helz, R. T., Thornber, C. R. Geothermometry of Kilauea Iki lava lake, Hawaii. Bulletin of Volcanology, 49 (5), p. 651-668. 1987.

Hofmann, A. W., Mantle plumes from ancient oceanic crust. Earth and Planetary Science Letters, 57 (2), p. 421-436. 1982.

Jackson, M. C., Frey, F. A., Garcia, M. O., Wilmoth, R. A. Geology and geochemistry of basaltic lava flows and dikes from the Trans-Koolau Tunnel, Oahu, Hawaii. Bulletin of Volcanology, 60 (5), p. 381-401. 1999.

Jakobsson, S. P. On the consolidation and palagonitization of the tephra of the Surtsey volcanic island, Iceland. Surtsey Research Program Report (6), p. 121-128. 1972.

Jarosewich, E., Nelen, J. A., Norberg, J. A. Electron microprobe reference samples for mineral analyses. Fudali, R. F. (ed.). Mineral sciences investigations; 1976-1977. Smithsonian Contributions to the Earth Sciences (22), p. 68-69. 1979.

Lanphere, M. A., Dalrymple, G. B. Age and strontium isotopic composition of the Honolulu Volcanic Series, Oahu, Hawaii. Irving, A. J., Dungan, M. A. (eds). The Jackson volume, American Journal of Science, Vol. 280-A (Part 2), p. 736-751. 1980.

Lassiter, J. C. & Hauri, E. H. Osmium-isotope variations in Hawaiian lavas; evidence for recycled oceanic lithosphere in the Hawaiian Plume. Earth and Planetary Science Letters, 164 (3-4), p. 483-496. 1998.

Le Maitre, R. W. (editor), Bateman, P., Dudek, A., Keller, J., Lemeyre, J., Le Bas, M. J., Sabine, P. A., Schmid, R., Sorensen, H., Streckeisen, A., Wooley, A. R., Zanettin, B. A classification of igneous rocks and glossary of terms, p. 193. 1989.

Lipman, P. W., Rhodes, J. M., Dalrymple, G. B. The Ninole Basalt; implications for the structural evolution of Mauna Loa Volcano, Hawaii. Bulletin of Volcanology, 53 (1), p. 1-19. 1990.

Macdonald, G. A., Abbott, A. T., Peterson, F.L. Volcanoes in the Sea, the geology of Hawaii. Second Edition. 1983.

Macdonald, G. A. Geology and geophysics of Hawaii. Geology and solid earth geophysics of the Pacific Basin. Proceedings of the Pacific Science Congress, p. 127-133. 1963.

Moore, J. G., Normark, W. R., Holcomb, R. T. Giant Hawaiian underwater landslides. Science, 264 (5155), p. 46-47. 1994.

Moore, J. G, Clague, D. A. Volcano growth and evolution of the Island of Hawaii; with Suppl. Data 92-34. Geological Society of America Bulletin, 104 (11), p. 1471-1484, 1992.

Moore, J. G., Clague, D. A., Holcomb, R. T., Lipman, P. W., Normark, W. R., Torresan, M. E. Prodigious submarine landslides on the Hawaiian Ridge. Journal of Geophysical Research, B, Solid Earth and Planets, 94 (12), p. 17,465-17,484. 1989.

Moore, J. G. Subsidence of the Hawaiian Ridge. Decker, R. W., Wright, T. L., Stauffer, P. H. (eds). Volcanism in Hawaii, U. S. Geological Survey Professional Paper, Chapter 2. P 1350, p. 85-100. 1987.

Multhaup, R. A. Subsurface Mapping of Basalts Based on Petrographic Characterization of Cuttings from Borehole Drilling on Oahu, Hawaii. Chapter 2, University of Hawaii Masters Thesis. P. 3-29. 1990.

Norman, M. D., Garcia, M. O., Kamenetsky, V. S., Nielsen, R. L. Olivine-hosted melt inclusions in Hawaiian picrites: equilibration, melting, and plume source characteristics. Chemical Geology, 183, p. 143-168. 2002.

Norman, M. D., Garcia, M. O. Primitive magmas and source characteristics of the Hawaiian Plume; petrology and geochemistry of shield picrites. Earth and Planetary Science Letters, 168 (1-2), p. 27-44. 1999.

Norrish, K., Hutton, J. T. An accurate x-ray spectrographic method for the analysis of a wide range of geological samples. Geochimica et Cosmochimica Acta, 33 (4), p. 431-453. 1969.

Ocean Drilling Program. Shipboard scientist's handbook, technical note no. 3. Texas A&M University. 1990.

Presley, T. K., Sinton, J. M., Pringle, M. Postshield volcanism and catastrophic mass wasting of the Waianae Volcano, Oahu, Hawaii. Bulletin of Volcanology, 58 (8), p. 597-616. 1997.

Quane, S. L., Garcia, M. O., Guillou, H., Hulsebosch, T. P. Magmatic history of the East Rift Zone of Kilauea Volcano, Hawaii based on drill core from SOH 1. Journal of Volcanology and Geothermal Research, 102 (3-4), p. 319-338. 2000.

Rhodes, J. M. Geochemical stratigraphy of lava flows sampled by the Hawaii Scientific Drilling Project, Journal of Geophysical Research, B, Solid Earth and Planets, 101 (5), p. 11,729-11,746. 1996.

Roden, M. F., Trull, T., Hart, S. R., Frey, F. A. New He, Nd, Pb, and Sr isotopic constraints on the constitution of the Hawaiian plume; results from Koolau Volcano, Oahu, Hawaii, USA. Geochimica et Cosmochimica Acta, 58 (5), p. 1431-1440. 1994.

Roden, M. F., Frey, F. A., Clague, D. A. Geochemistry of tholeiitic and alkalic lavas from the Koolau Range, Oahu, Hawaii; implications for Hawaiian volcanism. Earth and Planetary Science Letters, 69 (1), p. 141-158. 1984.

Sackett, Penelope C., McConnell, Vicki S., Roach, Angela L., Priest, Susan S., and Sass, John H. Long Valley Coring Project, Inyo County, California, 1998; preliminary stratigraphy and images of recovered core. Open-File Report - U. S. Geological Survey , OF 99-0158. 1999.

Satake, K., Smith, J. R., Shinozaki, K. Volume estimate and tsunami modeling for the Nuuanu and Wailau landslides. Geophysical Monograph 128: Evolution of Hawaiian Volcanoes, p. 333. 2002.

Shinozaki, Z.R., Ren, Z., Takahashi, E. Geochemical and Petrological Characteristics of Nuuanu and Wailau landslide blocks. Geophysical Monograph 128: Evolution of Hawaiian Volcanoes, p. 297. 2002.

Sinton, C. W., Christie, D. M., Duncan, R. A. Geochronology of Galapagos seamounts. Journal of Geophysical Research, B, Solid Earth and Planets, 101 (6), p. 13,689-13,700. 1996.

Sobolev, A. V., Hofmann, A.W., Nikogosian, I.K. Recycled oceanic crust observed in 'ghost plagioclase' within the source of Mauna Loa lavas. Nature, (London) 404, p. 986-989. 2000.

Stearns, H. T. Geologic map and guide of the Island of Oahu, Hawaii [with a chapter on mineral resources]. Bulletin - State of Hawaii, Division of Hydrography, p. 75, 7 pls. 1939.

Stearns, H. T., Vaksvik, K. N. Geology and ground-water resources of the island of Oahu, Hawaii. Bulletin - State of Hawaii, Division of Hydrography, p. 479. 1935.

Stille, P., Unruh, D. M., Tatsumoto, M. Pb, Sr, Nd and Hf isotopic evidence of multiple sources for Oahu, Hawaii basalts. Nature (London), 304 (5921), p. 25-29. 1983.

Takahashi, E., Nakajima, K. Melting Process in the Hawaiian Plume: An Experimental Study. Geophysical Monograph 128: Evolution of Hawaiian Volcanoes, p. 403. 2002.

Takeguchi, R., Takahashi, E. Primary Magma Composition in Koolau Volcano, Hawaii. In review.

Tanaka, R. Nakamura, E., Takahashi, E. Geochemical evolution of Koolau volcano, Hawaii. AGU Monograph 128: Evolution of Hawaiian Volcanoes, p. 311. 2002.

Trusdell, Frank A., Novak, Elizabeth, and Evans, S. Rene. Core lithology, State of Hawaii Scientific Observation Hole 4, Kilauea Volcano, Hawaii. Open-File Report - U. S. Geological Survey, OF 92-0586. 1992.

Walker, G. P. L. "Coherent intrusion complexes" in large basaltic volcanoes; a new structural model. Cox, K. G. & Baker, P. E. (eds.). Essays on magmas and other earth fluids; a volume in appreciation of Prof. Peter G. Harris. Journal of Volcanology and Geothermal Research, 50 (1-2), p. 41-54. 1992.

Walker, G. P. L. Geology and volcanology of the Hawaiian Islands. Pacific Science, 44 (4), p. 315-347. 1990.

Walker, G. P. L., Garcia, M.O. Koolau Lava-Shield Volcano. Field trip guide, Geological Society of America 83rd Annual Meeting, Cordilleran Section. 1987.

Walker, G. P. L. Koolau dike complex, Oahu; intensity and origin of a sheeted-dike complex high in a Hawaiian volcanic edifice. Geology (Boulder), 14 (4), p. 310-313. 1986.

Wentworth, C. K. Geology and ground-water resources of the Honolulu-Pearl Harbor area, Oahu, Hawaii. Honolulu, Hawaii Board Water Supply, p. 111. 1951.
Wentworth, C. K., Winchell, H. Koolau basalt series, Oahu, Hawaii. Geological Society of America Bulletin, 58 (1), p. 49-77. 1947.

Wentworth, C. K., Jones, A. E. Intrusive rocks of the leeward slope of the Koolau Range, Oahu. Journal of Geology, 48 (8, Part 2), p. 975-1006. 1940.

Winchell, H. Honolulu series, Oahu, Hawaii. Geological Society of America Bulletin, 58 (1), p. 1-48. 1947.

Wright, T. L., Fiske, R. S. Origin of the differentiated and hybrid lavas of Kilauea volcano, Hawaii. Journal of Petrology, 12 (1), p. 1-65. 1971.

Yaxley, G. M., Green, D.H. Reactions between eclogite and peridotite: mantle refertilisation by subduction of oceanic crust. Schweiz. Mineral. Petrogr. Mitt., 78, p. 243-255. 1998.